Δ_{33}-isobar contribution to the soft nucleon-nucleon potentials. I. 2π-exchange potentials

Th. A. Rijken* and V. G. J. Stoks

Institute for Theoretical Physics, University of Nijmegen, Nijmegen, The Netherlands

(Received 19 December 1991)

Two-pion-exchange (TPE) nucleon-nucleon potentials are derived for one or two Δ isobars in the intermediate states. Strong dynamical pair suppression is assumed. At the $NN\pi$ and the $N\Delta\pi$ vertices Gaussian form factors are incorporated into the relativistic two-body framework by using a dispersion representation for the one-pion-exchange amplitudes. The Fourier transformations are performed using factorization techniques for the energy denominators, taking into account the mass difference between the nucleon and the Δ isobar. Analytic expressions for the TPE potentials are obtained, which contain at most one-dimensional integrals. The TPE potentials are first calculated up to orders $(f_{NN\pi}f_{N\Delta\pi})^2$ and $f_{N\Delta\pi}^4$. These come from the adiabatic contributions of all planar and crossed three-dimensional momentum-space TPE diagrams. We also give the contributions of the OPE iteration, which can be subtracted or not, depending on whether one performs a coupled-channel calculation for, e.g., the $NN, N\Delta$ system, or a single NN-channel calculation. Next, we calculate the (m_π/M) corrections. These are due to the $1/M$ terms in the pion-nucleon vertices, and the $1/M$ terms in the nonadiabatic expansion of the nucleon energies in the intermediate states.

PACS number(s): 13.75.Cs, 21.30.+y, 12.40.Qq

I. INTRODUCTION

Recently, we have developed techniques to calculate the two-pion-exchange (TPE) nucleon-nucleon (NN) potentials for Gaussian form factors in an elegant fashion [1]. This makes it possible to study TPE in NN in the same approach and using the same type of parameters as in the Nijmegen soft-core one-boson-exchange OBE model [2, 3]. In this paper we extend the work of [1] to include the first Δ isobar and we calculate the 2π-exchange potentials (TPEP's) due to one and two Δ isobars in the intermediate states. Below we give a brief account of our approach and refer the interested reader for more of the relevant background to [1]. In the companion paper [4] we calculate the $\pi\rho$-exchange potential.

The investigation of the role of the Δ_{33} isobar in the nucleon-nucleon interaction and nuclear matter dates back to the 1960s and early 1970s. We limit our brief discussion to the potential-model approaches, since this provides the proper context for this paper. The early work involved the evaluation of $NN \leftrightarrow N\Delta, \Delta\Delta$ transitions and TPEP's in both configuration space and momentum space. Here we mention the work of Sugawara and von Hippel [5], Green and Haapakoski [6], Smith and Pandharipande [7], and a review on the early work on transition potentials [8]. For the dispersion relation approach of the Copenhagen, Paris, and Stony Brook groups, see Refs. [9–11]. From this work it was concluded that the $N\Delta$ mass difference cannot be neglected. The incorporation of this and other features can easily be achieved

by working in momentum space. Extensive work in momentum space has been done by the Bonn group, and for references and a review we refer to Ref. [12]. Also, the behavior of nucleons and Δ isobars in nuclear matter has been discussed by Malfliet and ter Haar [13] in the context of the Dirac-Brueckner theory. For a study of the role of the Δ isobar in the NN interaction using the Bethe-Salpeter equation, see the paper by van Faassen and Tjon [14]. A recent treatment using phenomenological transition and TPE potentials, with an emphasis on the inelastic region was done by Lomon [15].

Although the momentum-space techniques have the advantage that the energy dependence can be handled without making certain approximations, we consider a configuration-space treatment useful and to a certain extent complementary. In configuration space the Coulomb interaction and many other electromagnetic effects can be included easily in an accurate way. Furthermore, the physical interpretation of the effects on wave functions, phase parameters, etc., in terms of central, spin-spin, tensor, and spin-orbit potentials is very instructive. In this paper we show how to incorporate the $N\Delta$ mass difference properly in the configuration-space calculation. Also, the energy dependence is included in our treatment of the once-iterated graphs and the second-order Born terms.

We start the derivation of the TPEP from the relativistic coupled-channel two-body equations [16–18], where the interaction kernel is given by the two-baryon-irreducible Feynman diagrams. These are the diagrams with at most two pions in the intermediate states. The channel space includes the NN, the $N\Delta$, and the $\Delta\Delta$ channel. So, in principle, with our techniques we could calculate the TPEP's for such a complicated system. We will not carry through such a complete treatment in this

paper, but will restrict ourselves to the TPEP in the NN sector. After that, the derivation of the TPEP for the complete coupled-channel system will be obvious to the reader. To proceed from the four-dimensional relativistic equations to the three-dimensional equations, we apply the procedure of Salpeter [19] to the relativistic two-body (two-nucleon) equation by performing the energy integrations. Completely analogous to Ref. [1] this leads to the three-dimensional integral equation of Thompson [20], a definition of the interaction kernel, and a definition of the wave function.

In general, of course, one is unable to perform the energy integrations needed to derive the three-dimensional equations, and certain approximations are necessary. The particular approach we used in this matter [1] was given by Klein [21]. Actually, in the derivation of the TPEP's we may restrict ourselves to reproduce the Feynman graphs up to second order in the exchange and so we need in reality the Klein ansatz only to the free two-body wave function, where this is easily seen to be correct. In [1] we have shown that in this way we arrive at the "old-fashioned perturbation" diagrams in a straigthforward and unambiguous way.

The procedure to include the Gaussian form factors is exactly the same as in [1]. We generalize the results for pointlike vertices for the presence of the Gaussian form factors by employing the Lehmann spectral representation of the one-pion-exchange (OPE) amplitude. Then the generalization from the point coupling to the coupling with a form factor down to the level of the "old-fashioned perturbation" diagrams is easily derived.

To perform the analytic derivation of our formulas, we extend the technique used by us in [1] to account for the mass difference between the nucleon and the Δ isobar. This is particularly important for the treatment of the denominators coming from the intermediate states. Remarkably, also here it appeared feasible to carry through a complete factorization of the two-pion exchanges, albeit in most cases at the cost of one-dimensional integrals. This enables us to express the potentials in terms of one-dimensional integrals over products of the OPE functions already given in Ref. [2].

The diagrams we calculate are (i) the parallel and crossed TPE diagrams of the type that were calculated by Brueckner and Watson (BW) for nucleons in the intermediate states [22]; and (ii) the iterated OPE diagrams of the type that were calculated by Taketani, Machida, and Ohnuma (TMO) for nucleons in the intermediate states [23]. Although these calculations were generalized in Ref. [1] using Gaussian form factors at the vertices instead of point couplings, we still referred to the potentials as the BW and TMO potentials. As this distinction was convenient as a means to denote the different contributions, we will adopt this nomenclature also in this paper.

As in Ref. [1], we adopt the working hypothesis that in nature there is a "strong pair suppression" (see, e.g., Ref. [24]). In fact, we simply neglect the transitions from positive-energy to negative-energy states completely. One might assume that there exists a covariant phenomenological prescription to implement such strong

suppression arbitrarily close. Although pair diagrams are totally absent in this work due to our assumption, our techniques are, as will be clear from the sequel, fully adequate to treat also the pair diagrams and there technically is no impediment to include these diagrams.

The paper is organized as follows. In Sec. II the general approach within the framework of relativistic quantum mechanics is presented. Here the multichannel approach is presented and the decomposition of the Feynman propagator in positive- and negative-energy poles is given. In Sec. III the connection between the relativistic two-body equation description and that of the three-dimensional formalism is reviewed. In Sec. IV we derive the two-pion-exchange kernels for point interactions, which are then implemented with the various different form factors that occur. The definition of the TPEP for the Lippmann-Schwinger equation is given and the adiabatic expansion of the energy denominators from the intermediate states is discussed.

In Sec. V, using Appendices B and C, the TPEP's for the BW graphs and the TMO graphs are derived for the $N\Delta$ and $\Delta\Delta$ intermediate states. The TPE potentials are calculated up to orders $(f_{NN\pi}f_{N\Delta\pi})^2$ and $f_{N\Delta\pi}^4$. We also present the once-iterated OPE kernels for the $N\Delta$ and $\Delta\Delta$ graphs. These can be subtracted or not, depending on whether one performs a coupled-channel calculation for, e.g., the NN, $N\Delta$ system, or a single NN-channel calculation. In Sec. VI, (m_π/M) corrections due to the $1/M$ terms in the pion-nucleon vertices and the $1/M$ terms in the nonadiabatic expansion of the nucleon energies in the intermediate states are evaluated. Finally, in Sec. VII the results are shown and discussed.

In carrying through the calculations, we have ignored purely off-energy-shell contributions to the potentials. In principle these could be included as well, but this would make the algebra more cumbersome. Moreover, we do not distinguish between the different nucleon masses (collectively denoted by M) or between the different pion masses and coupling constants, hence our results are SU(2) symmetric. The (average) pion mass is denoted by m_π.

In Appendix A the treatment of the energy denominator of the intermediate state of the TMO graphs is discussed. In Appendix B the procedure to include the Gaussian form factor is described and demonstrated. In particular, here the factorization technique for the energy denominators is extended to include the mass difference between the nucleon and the Δ isobar. In Appendix C we indicate how the different characteristic potential forms emerge and we introduce a notation which makes it possible to present our results in a succinct manner.

II. RELATIVISTIC TWO-BODY EQUATIONS

We consider the coupled NN, $N\Delta$, and $\Delta\Delta$ channels

$$N_a(p_a, s_a) + N_b(p_b, s_b) \longleftrightarrow N_{a'}(p_{a'}, s_{a'}) + N_{b'}(p_{b'}, s_{b'})$$
$$\longleftrightarrow N_{a'}(p_{a'}, s_{a'}) + \Delta_{b'}(p_{b'}, s_{b'})$$
$$\longleftrightarrow \Delta_{a'}(p_{a'}, s_{a'}) + \Delta_{b'}(p_{b'}, s_{b'}).$$

Introducing the total and relative four-momentum for the initial and final states

$$P = p_a + p_b \ , \quad p = \tfrac{1}{2}(p_a - p_b) \ ,$$

$$P' = p_{a'} + p_{b'} \ , \quad p' = \tfrac{1}{2}(p_{a'} - p_{b'}) \ , \tag{2.1}$$

we have in the center-of-mass system (c.m. system) for a and b on-mass shell

$$P = (W, \mathbf{0}), \quad p = (0, \mathbf{p}), \quad p' = (0, \mathbf{p}'). \tag{2.2}$$

In general, the particles are off-mass-shell in the Green's functions. In the following, the on-mass-shell momenta for the initial and final states are denoted by p_i and p_f, respectively. Hence, $p_a^0 = E_a(\mathbf{p}_i) = (\mathbf{p}_i^2 + M_a^2)^{1/2}$ and $p_{a'}^0 = E_{a'}(\mathbf{p}_f) = (\mathbf{p}_f^2 + M_{a'}^2)^{1/2}$, and similarly for b and b'. Due to translation invariance, $P = P'$ and

$$W = W' = E_a(\mathbf{p}_i) + E_b(\mathbf{p}_i) = E_{a'}(\mathbf{p}_f) + E_{b'}(\mathbf{p}_f) \ .$$

The relativistic two-body scattering equation reads

$$\psi(p, P) = \psi^0(p, P) + G(p; P) \int d^4 p' \, I(p, p') \psi(p', P) \ , \tag{2.3}$$

where $\psi(p, P)$ is a 4×4 matrix in Dirac space, and a 3-dimensional column in channel space. The interaction kernel I and the two-particle Green's function G are 3×3 matrices in channel space. We describe here the Δ isobar as a particle with a fixed mass using the Rarita-Schwinger formalism (see, e.g., Ref. [25]). Therefore, in the channels with a Δ there will be extra Lorentz indices, which will occasionally be suppressed in order not to have to distinguish the different two-particle channels explicitly. The contributions to the kernel $I(p, p')$ come from the two-baryon-irreducible Feynman diagrams. In writing Eq. (2.3) we have taken out an overall δ-function which signals the total four-momentum conservation.

The two-particle Green's function $G(p; P)$ in Eq. (2.3) is simply the product of the free propagators for the baryons of line (a) and (b). The nucleon and the Δ-isobar Feynman propagators are given by the well-known formula

$$G_{\{\mu\},\{\nu\}}^{(s)}(p) = \int d^4 x \, \langle 0 | T(\psi_{\{\mu\}}^{(s)}(x) \overline{\psi}_{\{\nu\}}^{(s)}(0)) | 0 \rangle \, e^{ip \cdot x}$$

$$= \frac{\Pi^s(p)}{p^2 - M^2 + i\delta} \ , \tag{2.4}$$

where $\psi_{\{\mu\}}^{(s)}$ are the free Rarita-Schwinger fields which describe the $s = \tfrac{1}{2}$ and $s = \tfrac{3}{2}$ baryons (see, e.g., Ref. [26]). For the nucleon $\{\mu\} = \emptyset$, while for the Δ isobar $\{\mu\} = \mu$. In terms of these one-particle Green's functions the two-particle Green's function in Eq. (2.3) reads

$$G(p; P) = \frac{i}{(2\pi)^4} \left[\frac{\Pi^{(s_a)}(\tfrac{1}{2}P + p)}{(\tfrac{1}{2}P + p)^2 - M_a^2 + i\delta} \right]^{(a)}$$

$$\times \left[\frac{\Pi^{(s_b)}(\tfrac{1}{2}P - p)}{(\tfrac{1}{2}P - p)^2 - M_b^2 + i\delta} \right]^{(b)} . \tag{2.5}$$

Using now a complete set of on-mass-shell spin-s states in the first line of Eq. (2.4), one finds that the Feynman propagator of a spin-s baryon off-mass-shell can be written as

$$\frac{\Pi^{(s)}(p)}{p^2 - M^2 + i\delta} = \frac{M}{E(\mathbf{p})}$$

$$\times \left[\frac{\Lambda_+^{(s)}(\mathbf{p})}{p_0 - E(\mathbf{p}) + i\delta} - \frac{\Lambda_-^{(s)}(-\mathbf{p})}{p_0 + E(\mathbf{p}) - i\delta} \right] , \tag{2.6}$$

where $E(\mathbf{p}) = (\mathbf{p}^2 + M^2)^{1/2}$ with M the nucleon or the Δ-isobar mass. $\Lambda_+^{(s)}(\mathbf{p})$ and $\Lambda_-^{(s)}(\mathbf{p})$ with $s = \tfrac{1}{2}$ or $\tfrac{3}{2}$ are the on-mass-shell projection operators on the positive- and negative-energy states. For the nucleon and for the Δ isobar they are respectively [27]

$$\Lambda_+^{(1/2)}(\mathbf{p}) = \sum_{\sigma=-1/2}^{+1/2} u(\mathbf{p}, \sigma) \otimes \bar{u}(\mathbf{p}, \sigma) \ ,$$

$$\Lambda_-^{(1/2)}(\mathbf{p}) = - \sum_{\sigma=-1/2}^{+1/2} v(\mathbf{p}, \sigma) \otimes \bar{v}(\mathbf{p}, \sigma) \ ,$$

$$\Lambda_+^{(3/2)}(\mathbf{p}) = \sum_{\sigma=-3/2}^{+3/2} u_\mu(\mathbf{p}, \sigma) \otimes \bar{u}_\nu(\mathbf{p}, \sigma) \ ,$$

$$\Lambda_-^{(3/2)}(\mathbf{p}) = - \sum_{\sigma=-3/2}^{+3/2} v_\mu(\mathbf{p}, \sigma) \otimes \bar{v}_\nu(\mathbf{p}, \sigma) \ ,$$

where u_μ and v_μ denote the Rarita-Schwinger spinors for spin-$\tfrac{3}{2}$ particles. Therefore, in the c.m. system, where $\mathbf{P} = 0$ and $P_0 = W$, the Green's function can be written as

$$G(p; W) = \frac{i}{(2\pi)^4} \left(\frac{M_a}{E_a(\mathbf{p})} \right) \left[\frac{\Lambda_+^{(s_a)}(\mathbf{p})}{\tfrac{1}{2}W + p_0 - E_a(\mathbf{p}) + i\delta} - \frac{\Lambda_-^{(s_a)}(-\mathbf{p})}{\tfrac{1}{2}W + p_0 + E_a(\mathbf{p}) - i\delta} \right]$$

$$\times \left(\frac{M_b}{E_b(\mathbf{p})} \right) \left[\frac{\Lambda_+^{(s_b)}(-\mathbf{p})}{\tfrac{1}{2}W - p_0 - E_b(\mathbf{p}) + i\delta} - \frac{\Lambda_-^{(s_b)}(\mathbf{p})}{\tfrac{1}{2}W - p_0 + E_b(\mathbf{p}) - i\delta} \right] . \tag{2.8}$$

Performing the multiplication in Eq. (2.8), we write the ensuing terms in shorthand notation as

$$G(p; W) = G_{++}(p; W) + G_{+-}(p; W)$$
$$+ G_{-+}(p; W) + G_{--}(p; W) ,$$

where, e.g., G_{++} corresponds to the term with $\Lambda_+^{s_a} \Lambda_+^{s_b}$. Introducing the wave functions (see Ref. [19])

$$\psi_{rs}(p') = \Lambda_r^{s_a} \Lambda_s^{s_b} \psi(p') \quad (r, s = +, -) , \quad (2.9)$$

the two-body equation (2.3) for ψ_{++} can be written as

$$\psi_{++}(p) = \psi_{++}^0(p) + G_{++}(p; W)$$
$$\times \int d^4 p' \sum_{r,s} I(p, p')_{++,rs} \psi_{rs}(p') , \quad (2.10)$$

and similar equations for ψ_{+-}, ψ_{-+}, and ψ_{--}.

Invoking "dynamical pair suppression," as discussed in Ref. [1], Eq. (2.10) reduces to a four-dimensional equation for ψ_{++}, i.e.,

$$\psi_{++}(p) = \psi_{++}^0(p) + G_{++}(p; W)$$
$$\times \int d^4 p' \, I(p, p')_{++,++} \psi_{++}(p') , \quad (2.11)$$

with the Green's function

$$G_{++}(p; W)_{\beta,\alpha} = \frac{i \delta_{\beta,\alpha}}{(2\pi)^4} \left[\frac{M_a M_b}{E_a(\mathbf{p}) E_b(\mathbf{p})} \right] \Lambda_+^{s_a}(\mathbf{p}) \Lambda_+^{s_b}(-\mathbf{p})$$
$$\times \left[\tfrac{1}{2} W + p_0 - E_a(\mathbf{p}) + i\delta \right]^{-1}$$
$$\times \left[\tfrac{1}{2} W - p_0 - E_b(\mathbf{p}) + i\delta \right]^{-1} , \quad (2.12)$$

where α and β are channel indices.

III. MULTICHANNEL THREE-DIMENSIONAL INTEGRAL EQUATIONS

Following the same procedures as in Ref. [1], we introduce the three-dimensional multichannel wave function according to Salpeter [19] by

$$\phi(\mathbf{p}) = \sqrt{\frac{E_a(\mathbf{p}) E_b(\mathbf{p})}{M_a M_b}} \int_{-\infty}^{\infty} \psi(p_\mu) dp_0 . \quad (3.1)$$

Using the approach of Klein [21], we make the ansatz

$$\psi(p'_\mu) = \sqrt{\frac{M_a M_b}{E_a(\mathbf{p}') E_b(\mathbf{p}')}} A_W(p'_\mu) \phi(\mathbf{p}') ,$$
$$A_W(p'_\mu) = -\frac{1}{2\pi i} \frac{W - \mathcal{W}(\mathbf{p}')}{F_W^{(a)}(\mathbf{p}', p'_0) F_W^{(b)}(-\mathbf{p}', -p'_0)} .$$

Here we used the notations

$$F_W(\mathbf{p}, p_0) = \tfrac{1}{2} W + p_0 - E(\mathbf{p}) + i\delta ,$$
$$\mathcal{W}(\mathbf{p}) = E_a(\mathbf{p}) + E_b(\mathbf{p}) .$$

Then, after performing the p_0 and p'_0 integration in Eq. (2.11) one arrives at the multichannel Thompson equation [20]

$$\phi_{++}(\mathbf{p}') = \phi_{++}^{(0)}(\mathbf{p}') + E_2^{(+)}(\mathbf{p}'; W)$$
$$\times \int d^3 p \, K^{\mathrm{irr}}(\mathbf{p}', \mathbf{p}|W) \, \phi_{++}(\mathbf{p}) , \quad (3.2)$$

where now the Green's function is

$$E_2^{(+)}(\mathbf{p}'; W)_{\beta,\alpha} = \frac{\delta_{\beta,\alpha}}{(2\pi)^3} \frac{\Lambda_+^a(\mathbf{p}') \Lambda_+^b(-\mathbf{p}')}{W - \mathcal{W}(\mathbf{p}') + i\delta} , \quad (3.3)$$

and where again α and β are channel indices. The kernel is given by

$$K^{\mathrm{irr}}(\mathbf{p}', \mathbf{p}|W) = -\frac{1}{(2\pi)^2} \sqrt{\frac{M_a M_b}{E_a(\mathbf{p}') E_b(\mathbf{p}')}} \left[W - \mathcal{W}(\mathbf{p}') \right] \left[W - \mathcal{W}(\mathbf{p}) \right] \sqrt{\frac{M_a M_b}{E_a(\mathbf{p}) E_b(\mathbf{p})}} \int_{-\infty}^{+\infty} dp'_0 \int_{-\infty}^{+\infty} dp_0$$

$$\times \left\{ \left[F_W^{(a)}(\mathbf{p}', p'_0) F_W^{(b)}(-\mathbf{p}', -p'_0) \right]^{-1} [I(p'_0, \mathbf{p}'; p_0, \mathbf{p})]_{++,++} \left[F_W^{(a)}(\mathbf{p}, p_0) F_W^{(b)}(-\mathbf{p}, -p_0) \right]^{-1} \right\} . \quad (3.4)$$

The M/E factors in Eq. (3.4) are due to the difference between the relativistic and the nonrelativistic normalization of the two-particle states. In the following we simply put $M/E(\mathbf{p}) = 1$ in the kernel. The corrections to this approximation would give $(m_\pi/M)^2$ corrections to the potentials, which we neglect.

The contributions to the two-particle irreducible kernel K^{irr} up to second order in the meson exchange are given by single- and double-meson exchange. For the definition of the TPE potential in the Lippmann-Schwinger equation we shall need the complete fourth-order kernel for the Thompson equation (3.2). In operator notation,

we have from Eq. (3.2)

$$\phi_{++} = \phi_{++}^{(0)} + E_2^{(+)} K^{\mathrm{irr}} \phi_{++}$$
$$= \phi_{++}^{(0)} + E_2^{(+)} \left(K^{\mathrm{irr}} + K^{\mathrm{irr}} E_2^{(+)} K^{\mathrm{irr}} + \cdots \right) \phi_{++}^{(0)}$$
$$\equiv \left(1 + E_2^{(+)} K \right) \phi_{++}^{(0)} , \quad (3.5)$$

which implies for the complete kernel K the integral equation

$$K(\mathbf{p'}, \mathbf{p}|W) = K^{\mathrm{irr}}(\mathbf{p'}, \mathbf{p}|W)$$
$$+ \int d^3 p'' K^{\mathrm{irr}}(\mathbf{p'}, \mathbf{p''}|W)$$
$$\times E_2^{(+)}(\mathbf{p''}; W) K(\mathbf{p''}, \mathbf{p}|W) . \quad (3.6)$$

Note that diagram (a) of Fig. 1 is generated from the iterated one-pion exchange in Eq. (3.6), albeit with the Thompson two-particle propagator of Eq. (3.3).

IV. NUCLEON-NUCLEON TWO-MESON EXCHANGE

In the first part of this section we calculate the complete kernel $K(\mathbf{p'}, \mathbf{p}; W)$ for the nucleon-nucleon sector only. In the second part we define the potential $V(\mathbf{p'}, \mathbf{p}; W)$ such that up to second-order meson exchange the Thompson amplitude is recovered completely when using this potential in the Lippmann-Schwinger equation. Although we deal with 2π-exchange only in this paper, we keep the discussion partly general such as to apply also to $\pi\rho$ exchange, which will be dealt with in the companion paper [4].

A. The nucleon-nucleon kernel

For convenience, we multiply each baryon-baryon-meson (BBM) vertex by a factor λ, which in the end will be set equal to 1. In the calculation of the interaction kernel, we restrict ourselves to terms up to and including the fourth order in λ. Writing the wave function as a series in λ, and the interaction kernel as a sum of the second- and the fourth-order term, we have

$$\phi_{++}(\mathbf{p'}) = \phi_{++}^{(0)}(\mathbf{p'}) + \lambda^2 \phi_{++}^{(2)}(\mathbf{p'}) + \lambda^4 \phi_{++}^{(4)}(\mathbf{p'}) + \cdots$$
$$K(\mathbf{p'}, \mathbf{p}|W) = \lambda^2 K^{(2)}(\mathbf{p'}, \mathbf{p}|W) + \lambda^4 K^{(4)}(\mathbf{p'}, \mathbf{p}|W) .$$
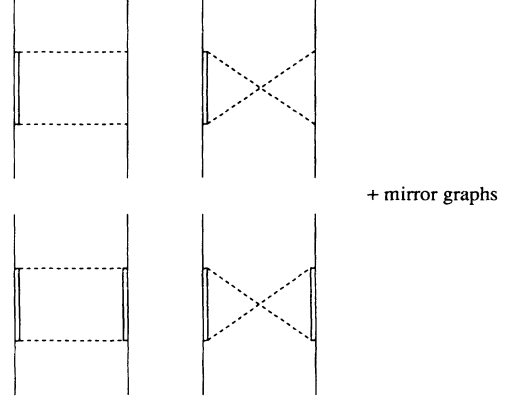
FIG. 1. Feynman diagrams for two-pion exchange with (a) one or (b) two Δ_{33} isobars in the intermediate states.

From Eq. (3.6) one sees that, written in operator notation,

$$K^{(2)} = K^{\mathrm{irr}(2)} ,$$
$$K^{(4)} = K^{\mathrm{irr}(4)} + K^{\mathrm{irr}(2)} E_2^{(+)} K^{\mathrm{irr}(2)} ,$$

and so the $K^{(2)}$ term corresponds to the OPE Feynman diagram, whereas the $K^{(4)}$ term corresponds to the graphs in Fig. 1. From Eq. (3.5) we then find for the wave function

$$\phi_{++}^{(2)} = E_2^{(+)} K^{\mathrm{irr}(2)} \phi_{++}^{(0)} ,$$
$$\phi_{++}^{(4)} = E_2^{(+)} \left[K^{\mathrm{irr}(2)} E_2^{(+)} K^{\mathrm{irr}(2)} + K^{\mathrm{irr}(4)} \right] \phi_{++}^{(0)} .$$

In this paper we exclusively deal with the fourth-order λ terms, which correspond to the Feynman diagrams of Fig. 1. These fourth-order Feynman diagrams, the so-called planar-box and crossed-box diagram, lead to the following expression for the fourth-order kernel:

$$K^{(4)}(\mathbf{p'}, \mathbf{p}|W)_{a'b';ab} = -(2\pi)^{-2} [W - \mathcal{W}(\mathbf{p'})][W - \mathcal{W}(\mathbf{p})] \sum_{a'', b''} \int dp'_0 \int dp_0 \int dk'_0 \int dk_0 \int d\mathbf{k'} \int d\mathbf{k}$$

$$\times i(2\pi)^{-4} \delta^4(p - p' - k - k')[k'^2 - m^2 + i\delta]^{-1} \left[F_W^{(a')}(\mathbf{p'}, p'_0) F_W^{(b')}(-\mathbf{p'}, -p'_0) \right]^{-1}$$

$$\times \{ [\Gamma_j \, F_W^{-1}(\mathbf{p} - \mathbf{k}, p_0 - k_0) \, \Gamma_i]^{(a'')} [\Gamma_j \, F_W^{-1}(-\mathbf{p} + \mathbf{k}, -p_0 + k_0) \, \Gamma_i]^{(b'')}$$

$$+ [\Gamma_j \, F_W^{-1}(\mathbf{p} - \mathbf{k}, p_0 - k_0) \, \Gamma_i]^{(a'')} [\Gamma_i \, F_W^{-1}(-\mathbf{p'} - \mathbf{k}, -p'_0 - k_0) \, \Gamma_j]^{(b'')} \}$$

$$\times \left[F_W^{(a)}(\mathbf{p}, p_0) F_W^{(b)}(-\mathbf{p}, -p_0) \right]^{-1} [k^2 - m^2 + i\delta]^{-1} . \quad (4.1)$$

Here $a, a', a'' = N, \Delta$ and $b, b', b'' = N, \Delta$, where a'' and b'' denote the baryons of the intermediate state. The initial baryons a, b and the final baryons a', b' depend, of course, on the particular transition. We have indicated the c.m. momenta for the planar and crossed diagram

in Fig. 2. Note that the first term between the curly brackets corresponds to the planar-box diagram and the second term to the crossed-box diagram in Fig. 1. In Eq. (4.1), Γ_i and Γ_j denote the BBM vertices. They follow from the interaction Lagrangians. The expression

(a)

FIG. 3. Planar BW two-pion-exchange potential graphs with one Δ_{33} isobar in the intermediate state.

(b)
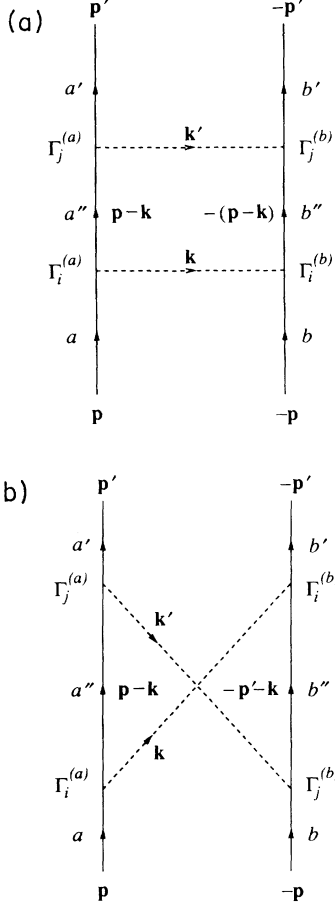
FIG. 2. Definition of momentum vectors in second-order (a) planar and (b) crossed graphs.
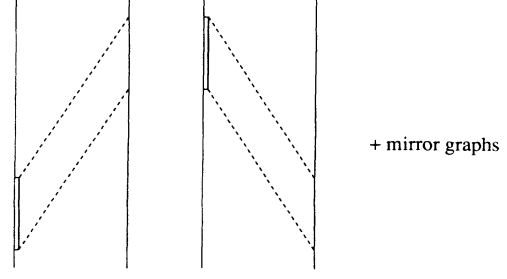
between curly brackets is the fourth-order contribution in λ to the kernel $I(p';p)_{++,++}$. In the latter we use the $N\Delta$ or the $\Delta\Delta$ Green's function (2.12) for the intermediate states. Also we have put here $M/E = 1$.

So far our discussion has been quite general. From now on we restrict ourselves to the nucleon-nucleon sector and henceforth specialize to the TPE potentials which are actually derived in this paper. From the explicit expression in Eq. (4.1) it is clear that one can perform the integration over the energy variables p'_0, p_0, and k_0. The execution of these integrations is quite similar to those worked out explicitly in [1], as are the results. To illustrate the results we restrict ourselves to the graphs of Figs. 3–5. Those for the mirror graphs can be readily obtained by inspection of these graphs. The results for the planar- and crossed-box diagram are as follows.

(i) The planar-box diagram. Here we encounter the integral

$$I_{//}(\mathbf{p}',\mathbf{p}|W) = [W - \mathcal{W}(\mathbf{p}')]\,[W - \mathcal{W}(\mathbf{p})]\int dp'_0 \int dp_0 \int dk_0\,[(p - p' - k)^2 - m^2 + i\delta]^{-1}$$

$$\times \left[F_W^{(a')}(\mathbf{p}',p'_0)F_W^{(b')}(-\mathbf{p}',-p'_0)\right]^{-1}\left[F_W^{(a'')}(\mathbf{p} - \mathbf{k},p_0 - k_0)F_W^{(b'')}(-\mathbf{p} + \mathbf{k},-p_0 + k_0)\right]^{-1}$$

$$\times \left[F_W^{(a)}(\mathbf{p},p_0)F_W^{(b)}(-\mathbf{p},-p_0)\right]^{-1}[k^2 - m^2 + i\delta]^{-1}\,,\tag{4.2}$$

which is treated in Ref. [1], to which we refer for details. There appear two contributions. For the $N\Delta$ intermediate state, the first corresponds to the planar BW diagrams of Fig. 3 and the second to the TMO diagrams of Fig. 5. Their contributions to the interaction kernel are

$$K_{\text{BW}_{//}}^{(3a)}(\mathbf{p}',\mathbf{p}|W) = -\frac{1}{(2\pi)^3}\int \frac{d^3k}{4\omega_{\mathbf{k}}\omega_{\mathbf{k}'}}\frac{[\Gamma_j\Lambda_+(\mathbf{p} - \mathbf{k})\Gamma_i]^{(a)}}{[\mathcal{E}_{\mathbf{p}-\mathbf{k}} + E_{\mathbf{p}} - W + \omega_{\mathbf{k}}]}\frac{[\Gamma_j\Lambda_+(-\mathbf{p} + \mathbf{k})\Gamma_i]^{(b)}}{[E_{\mathbf{p}'} + E_{\mathbf{p}-\mathbf{k}} - W + \omega_{\mathbf{k}'}]}$$

$$\times \frac{1}{[E_{\mathbf{p}} + E_{\mathbf{p}'} - W + \omega_{\mathbf{k}} + \omega_{\mathbf{k}'}]}\,,\tag{4.3}$$

$$K_{\text{TMO}}^{(5a)}(\mathbf{p}',\mathbf{p}|W) = -\frac{1}{(2\pi)^3}\int \frac{d^3k}{4\omega_{\mathbf{k}}\omega_{\mathbf{k}'}}\frac{[\Gamma_j\Lambda_+(\mathbf{p} - \mathbf{k})\Gamma_i]^{(a)}}{[\mathcal{E}_{\mathbf{p}-\mathbf{k}} + E_{\mathbf{p}} - W + \omega_{\mathbf{k}}]}\frac{[\Gamma_j\Lambda_+(-\mathbf{p} + \mathbf{k})\Gamma_i]^{(b)}}{[E_{\mathbf{p}'} + E_{\mathbf{p}-\mathbf{k}} - W + \omega_{\mathbf{k}'}]}$$

$$\times \frac{1}{[\mathcal{E}_{\mathbf{p}-\mathbf{k}} + E_{\mathbf{p}-\mathbf{k}} - W]}\,,\tag{4.4a}$$

$$K_{\text{TMO}}^{(5b)}(\mathbf{p}', \mathbf{p}|W) = -\frac{1}{(2\pi)^3} \int \frac{d^3k}{4\omega_{\mathbf{k}}\omega_{\mathbf{k}'}} \frac{[\Gamma_j \Lambda_+(\mathbf{p}-\mathbf{k})\Gamma_i]^{(a)}}{[\mathcal{E}_{\mathbf{p}-\mathbf{k}} + E_{\mathbf{p}} - W + \omega_{\mathbf{k}}]} \frac{[\Gamma_j \Lambda_+(-\mathbf{p}+\mathbf{k})\Gamma_i]^{(b)}}{[\mathcal{E}_{\mathbf{p}-\mathbf{k}} + E_{\mathbf{p}'} - W + \omega_{\mathbf{k}'}]}$$

$$\times \frac{1}{[\mathcal{E}_{\mathbf{p}-\mathbf{k}} + E_{\mathbf{p}-\mathbf{k}} - W]} , \tag{4.4b}$$

where $\omega = \sqrt{\mathbf{k}^2 + m^2}$ and $\omega' = \sqrt{\mathbf{k}'^2 + m^2}$ with $\mathbf{k}' \equiv \mathbf{p} - \mathbf{p}' - \mathbf{k}$. Also, we have denoted the energies of the nucleons by E and the energies of the Δ isobar by $\mathcal{E}$. Here we have to add the kernels of the graphs (a$'$) and (b$'$), and all mirror graphs. They merely contribute a total factor of four when we evaluate the potentials.

(ii) The crossed-box diagram. Here the integral to be performed is essentially

$$I_X(\mathbf{p}', \mathbf{p}|W) = [W - \mathcal{W}(\mathbf{p}')] [W - \mathcal{W}(\mathbf{p})] \int dp_0' \int dp_0 \int dk_0 \, [(p - p' - k)^2 - m^2 + i\delta]^{-1}$$

$$\times \left[F_W^{(a')}(\mathbf{p}', p_0') F_W^{(b')}(-\mathbf{p}', -p_0') \right]^{-1} \left[F_W^{(a'')}(\mathbf{p}-\mathbf{k}, p_0 - k_0) F_W^{(b'')}(-\mathbf{p}'-\mathbf{k}, -p_0' - k_0) \right]^{-1}$$

$$\times \left[F_W^{(a)}(\mathbf{p}, p_0) F_W^{(b)}(-\mathbf{p}, -p_0) \right]^{-1} [k^2 - m^2 + i\delta]^{-1} , \tag{4.5}$$

where for details we refer again to Ref. [1]. The results correspond to the crossed BW diagrams of Fig. 4, and the corresponding interaction kernels are

$$K_{\text{BW}_X}^{(4a)}(\mathbf{p}', \mathbf{p}|W) = -\frac{1}{(2\pi)^3} \int \frac{d^3k}{4\omega_{\mathbf{k}}\omega_{\mathbf{k}'}} \frac{[\Gamma_j \Lambda_+(\mathbf{p}-\mathbf{k})\Gamma_i]^{(a)}}{[\mathcal{E}_{\mathbf{p}-\mathbf{k}} + E_{\mathbf{p}} - W + \omega_{\mathbf{k}}]} \frac{[\Gamma_i \Lambda_+(-\mathbf{p}'-\mathbf{k})\Gamma_j]^{(b)}}{[E_{\mathbf{p}'} + E_{\mathbf{p}'+\mathbf{k}} - W + \omega_{\mathbf{k}}]}$$

$$\times \frac{1}{[E_{\mathbf{p}} + E_{\mathbf{p}'} - W + \omega_{\mathbf{k}} + \omega_{\mathbf{k}'}]} , \tag{4.6a}$$

$$K_{\text{BW}_X}^{(4b)}(\mathbf{p}', \mathbf{p}|W) = -\frac{1}{(2\pi)^3} \int \frac{d^3k}{4\omega_{\mathbf{k}}\omega_{\mathbf{k}'}} \frac{[\Gamma_j \Lambda_+(\mathbf{p}-\mathbf{k})\Gamma_i]^{(a)}}{[\mathcal{E}_{\mathbf{p}-\mathbf{k}} + E_{\mathbf{p}} - W + \omega_{\mathbf{k}}]} \frac{[\Gamma_i \Lambda_+(-\mathbf{p}'-\mathbf{k})\Gamma_j]^{(b)}}{[E_{\mathbf{p}'} + E_{\mathbf{p}'+\mathbf{k}} - W + \omega_{\mathbf{k}}]}$$

$$\times \frac{1}{[\mathcal{E}_{\mathbf{p}-\mathbf{k}} + E_{\mathbf{p}'+\mathbf{k}} - W + \omega_{\mathbf{k}} + \omega_{\mathbf{k}'}]} , \tag{4.6b}$$

$$K_{\text{BW}_X}^{(4c)}(\mathbf{p}', \mathbf{p}|W) = -\frac{1}{(2\pi)^3} \int \frac{d^3k}{4\omega_{\mathbf{k}}\omega_{\mathbf{k}'}} \frac{[\Gamma_j \Lambda_+(\mathbf{p}-\mathbf{k})\Gamma_i]^{(a)}}{[\mathcal{E}_{\mathbf{p}-\mathbf{k}} + E_{\mathbf{p}} - W + \omega_{\mathbf{k}}]} \frac{[\Gamma_i \Lambda_+(-\mathbf{p}'-\mathbf{k})\Gamma_j]^{(b)}}{[\mathcal{E}_{\mathbf{p}-\mathbf{k}} + E_{\mathbf{p}'} - W + \omega_{\mathbf{k}'}]}$$

$$\times \frac{1}{[\mathcal{E}_{\mathbf{p}-\mathbf{k}} + E_{\mathbf{p}'+\mathbf{k}} - W + \omega_{\mathbf{k}} + \omega_{\mathbf{k}'}]} . \tag{4.6c}$$
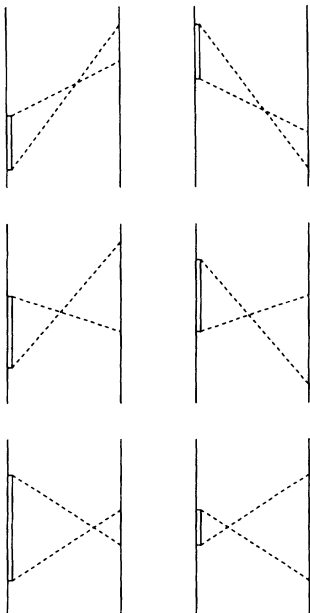
Here also we have to add the kernels from the graphs (a$'$), (b$'$), and (c$'$), and all their mirror graphs, which again merely gives rise to a factor of four when we evaluate the potentials.

The particular vertices we need for the TPEP in the

FIG. 4.   Crossed BW two-pion-exchange potential graphs with one Δ_{33} isobar in the intermediate state.

+ mirror graphs

+ mirror graphs
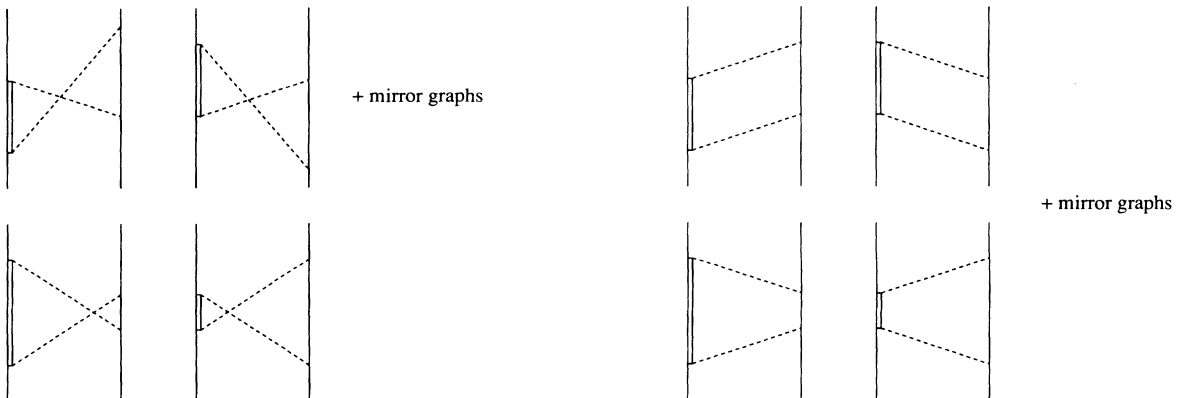
FIG. 5.   TMO two-pion-exchange potential graphs with one Δ_{33} isobar in the intermediate state.

nucleon-nucleon sector are the $NN\pi$ and the $N\Delta\pi$ vertex. Explicitly, for point couplings the relevant Lagrangians are

$$\mathcal{L}_{NN\pi} = \left(\frac{f_{NN\pi}}{m_\pi}\right) \bar{\psi}\gamma_5\gamma_\mu\tau\psi \cdot \partial^\mu\phi ,$$

$$\mathcal{L}_{N\Delta\pi} = \left(\frac{f_{N\Delta\pi}}{m_\pi}\right) \bar{\psi}\mathbf{T}\psi_\mu \cdot \partial^\mu\phi + \text{H.c.} ,$$

where $\mathbf{T}$ is the isospin-$\frac{1}{2}$ isospin-$\frac{3}{2}$ transition operator. In momentum space this gives for the $NN\pi$ vertex

$$\bar{u}(\mathbf{p}')\Gamma^{(a)}u(\mathbf{p}) = i\left(\frac{f_{NN\pi}}{m_\pi}\right) \bar{u}(\mathbf{p}')\gamma_5\gamma \cdot (p - p')u(\mathbf{p}) ,$$

and for the $N\Delta\pi$ vertex:

$$\bar{u}(\mathbf{p}')\Gamma_\mu^{(a)}u^\mu(\mathbf{p}) = i\left(\frac{f_{N\Delta\pi}}{m_\pi}\right) \bar{u}(\mathbf{p}')u_\mu(\mathbf{p}) \cdot (p - p')^\mu .$$

The generalization of the interaction kernels given above to the case with Gaussian form factors has been treated and explained in [1]. The same procedure can be used here and we will indicate only the minor changes in Eq. (4.1). For each OPE line in the Feynman propagator, we make the substitution

$$[k^2 - m^2 + i\delta]^{-1} \longrightarrow \int_0^\infty d\mu^2 \frac{\rho(\mu^2)}{k^2 - \mu^2 + i\delta} , \quad (4.7)$$

where in the right-hand side $\rho(\mu^2)$ is the spectral function, representing the form factors involved in OPE. In principle, $\rho(\mu^2)$ depends on whether we have an $NN \to N\Delta$ transition or an $NN \to \Delta\Delta$ transition.

At low and medium energy, we have to a very good approximation $t = k^2 \approx -\mathbf{k}^2 < 0$, and so for spacelike momentum transfers we can use Gaussian form factors $F(\mathbf{k}^2) = \exp(-\mathbf{k}^2/\Lambda^2)$, where Λ denotes the cutoff mass. Having Gaussian form factors, we make the substitution

$$\int_0^\infty d\mu^2 \frac{\rho(\mu^2)}{\mathbf{k}^2 + \mu^2} \longrightarrow \frac{F(\mathbf{k}^2)}{\mathbf{k}^2 + m^2} . \quad (4.8)$$

Since by exploiting our separation techniques in handling the $\mathbf{k}$ and $\mathbf{k}'$ dependence, the substitution (4.8) is an adequate recipe for the inclusion of the Gaussian (or any other) form factor in all cases.

Differentiating between an $NN\pi$ vertex and an $N\Delta\pi$ vertex by using

$$F_{NN\pi}(\mathbf{k}^2) = e^{-\mathbf{k}^2/2\Lambda_{NN\pi}^2}, \quad F_{N\Delta\pi}(\mathbf{k}^2) = e^{-\mathbf{k}^2/2\Lambda_{N\Delta\pi}^2} ,$$

we get for an $NN \to N\Delta$ transition in Eq. (4.8)

$$F(\mathbf{k}^2) = F_{NN\pi}(\mathbf{k}^2)F_{N\Delta\pi}(\mathbf{k}^2), \quad \Lambda^{-2} = (\Lambda_{NN}^{-2} + \Lambda_{N\Delta}^{-2})/2 ,$$

whereas for an $NN \to \Delta\Delta$ transition we have

$$F(\mathbf{k}^2) = F_{N\Delta\pi}^2(\mathbf{k}^2), \quad \Lambda = \Lambda_{N\Delta} .$$

B. The nucleon-nucleon potential

The multichannel Lippmann-Schwinger equation is given by

$$\phi_\alpha = \phi_\alpha^{(0)} + g_{\alpha,\beta} V_{\beta,\gamma} \phi_\gamma , \quad (4.9)$$

with the Green's function $g_{\alpha,\beta}$ given by

$$g(\mathbf{p}; W)_{\alpha,\beta} = \frac{\delta_{\alpha,\beta}}{(2\pi)^3} \Lambda_+^a(\mathbf{p})\Lambda_+^b(-\mathbf{p})\frac{M}{\mathbf{p}_i^2 - \mathbf{p}^2 + i\delta} . \quad (4.10)$$

The multichannel potential V, up to fourth order in λ, is defined such that to that order the wave function and the T matrix are the same as that generated by the multichannel Thompson equation. This implies for the potential V

$$V^{(2)} = K^{(2)}, \quad V^{(4)} = K^{(4)} - K^{(2)}g\, K^{(2)} . \quad (4.11)$$

These equations have to be taken to where the initial and final states are on the energy shell. The second-order potential $V^{(2)}$ is given by one-meson exchange taken on energy shell, which is then equivalent to the potential diagram (a) in Fig. 9. The fourth-order potential $V^{(4)}$ consists of two parts. The first part is represented by the fourth-order planar- and crossed-box BW diagrams. The second part is represented by the TMO diagrams, from which we have to subtract the once-iterated meson-exchange contribution, so

$$V_{\text{TMO}} = K_{\text{TMO}} - K^{(2)}g\, K^{(2)} , \quad (4.12)$$

which will be henceforth referred to as the TMO contribution, in analogy with the definition in Ref. [1]. The second (Born) term is pictured in diagram (a) in Fig. 9.

So much for the general multichannel approach. As stated before, in this paper we will largely restrict ourselves to the nucleon-nucleon sector. In that sector the initial and final states are restricted to two-nucleon states. Furthermore, in this paper we focus on the contributions to the NN potential due to the Δ_{33} isobar up to λ^4. This means that the only contributions to be considered are the planar- and crossed-box diagrams with at least one Δ isobar in the intermediate state. When the Lippmann-Schwinger equation is solved in the nucleon-nucleon sector only, the subtraction of the iterated-meson exchange does not apply and so $V^{(4)} = K^{(4)}$. For that purpose, in Sec. V C we give the once-iterated pion-exchange kernels. These should be added to the TMO potential of Eq. (4.12) in order to compensate for the subtraction.

For Eq. (4.9) the transition from Dirac spinors to Pauli spinors is given in Appendix C of Ref. [1]. There we derived the Lippmann-Schwinger equation

$$\chi(\mathbf{p}') = \chi^{(0)}(\mathbf{p}') + \tilde{g}(\mathbf{p}') \int d^3p\, \mathcal{V}(\mathbf{p}',\mathbf{p})\chi(\mathbf{p}) , \quad (4.13)$$

for the Pauli-spinor wave functions $\chi(\mathbf{p})$. The wave function $\chi(\mathbf{p})$ and the potential $\mathcal{V}(\mathbf{p}',\mathbf{p})$ in the Pauli-spinor space are defined by

$$\phi(\mathbf{p}) = \sum_{\sigma_a,\sigma_b} \chi_{\sigma_a\sigma_b}(\mathbf{p})\, u_a(\mathbf{p},\sigma_a)u_b(-\mathbf{p},\sigma_b) , \quad (4.14)$$

$$\chi_{\sigma_a'}^{(a)\dagger}\chi_{\sigma_b'}^{(b)\dagger} \mathcal{V} \chi_{\sigma_a}^{(a)}\chi_{\sigma_b}^{(b)} = \bar{u}_a(\mathbf{p}',\sigma_a')\bar{u}_b(-\mathbf{p}',\sigma_b')V(\mathbf{p}',\mathbf{p})$$
$$\times u_a(\mathbf{p},\sigma_a)u_b(-\mathbf{p},\sigma_b) . \quad (4.15)$$

Like in the derivation of the one-boson-exchange potentials [2, 3], we make the approximation

$$E(\mathbf{p}) = (\mathbf{p}^2 + M^2)^{1/2} \approx M + \mathbf{p}^2/2M$$

everywhere in the interaction kernels of Sec. V, which of course is fully justified for low energies only. As a consequence, we have a similar expansion of the on-shell energy

$$W = 2(\mathbf{p}_i^2 + M^2)^{1/2} \approx 2M + \mathbf{p}_i^2/M \ .$$

In contrast to these kinds of approximations, the full $\mathbf{k}^2$ dependence of the form factors is kept throughout the derivation of the TPEP. Note that the Gaussian form factors strongly suppress the high-momentum transfers. This means that the contribution to the potentials from intermediate states which are far off energy shell cannot be very large.

For the reduction of the TPEP from Dirac-spinor space to Pauli-spinor space, we use Eq. (2.7) for the Λ_+ operators, which leads to matrix elements of the vertex operators between positive-energy Dirac spinors. Using the aforementioned energy approximation, the vertex operators in Pauli-spinor space up to order $1/M$ read as follows. (i) $NN\pi$ vertices:

$$\bar{u}(\mathbf{p}')\Gamma^{(a)}(\mathbf{p}',\mathbf{p})u(\mathbf{p})$$

$$= +i\left(\frac{f_{NN\pi}}{m_\pi}\right)\left[\boldsymbol{\sigma}_1 \cdot \mathbf{k} \mp \frac{\omega}{2M_N}\boldsymbol{\sigma}_1 \cdot (\mathbf{p}' + \mathbf{p})\right],$$

$$(4.16)$$

$$\bar{u}(-\mathbf{p}')\Gamma^{(b)}(\mathbf{p}',\mathbf{p})u(-\mathbf{p})$$

$$= -i\left(\frac{f_{NN\pi}}{m_\pi}\right)\left[\boldsymbol{\sigma}_2 \cdot \mathbf{k} \mp \frac{\omega}{2M_N}\boldsymbol{\sigma}_2 \cdot (\mathbf{p}' + \mathbf{p})\right],$$

(ii) $N\Delta\pi$ vertices:

$$\bar{u}(\mathbf{p}')\Gamma_\mu^{(a)}(\mathbf{p}',\mathbf{p})u^\mu(\mathbf{p}) = -i\left(\frac{f_{N\Delta\pi}}{m_\pi}\right)\boldsymbol{\Sigma}_1^\dagger \cdot \mathbf{k} \ ,$$

$$(4.17)$$

$$\bar{u}(-\mathbf{p}')\Gamma_\mu^{(b)}(\mathbf{p}',\mathbf{p})u^\mu(-\mathbf{p}) = +i\left(\frac{f_{N\Delta\pi}}{m_\pi}\right)\boldsymbol{\Sigma}_2^\dagger \cdot \mathbf{k} \ ,$$

where always $\mathbf{k} \equiv \mathbf{p} - \mathbf{p}'$. For the Γ-matrix elements in Eq. (4.16) the upper sign applies for the creation and the lower sign for the absorption of the pion at the vertex. Note that for line (a) and line (b) we have used the subscripts 1 and 2 for the $\boldsymbol{\sigma}$ and the $\boldsymbol{\Sigma}$ operators, respectively.

The $\boldsymbol{\Sigma}$ operators are the spin-$\frac{1}{2}$ spin-$\frac{3}{2}$ transition operators (see, e.g., Refs. [26, 28]). Useful for the evaluation of the second-order diagrams are the relations

$$\sigma_j\sigma_i = \delta_{ij} + i\epsilon_{jik}\sigma_k \ ,$$

$$(4.18)$$

$$\Sigma_j|\sigma\rangle\langle\sigma|\Sigma_i^\dagger = \tfrac{2}{3}\delta_{ij} - \tfrac{i}{3}\epsilon_{jik}\sigma_k.$$

Products of this type will occur for each baryon line. Identical formulas hold for the isospin operators τ_i and $\mathbf{T}_i$, respectively, where $\mathbf{T}_i$ ($i = 1, 2, 3$) are the components of the isospin-$\frac{1}{2}$ isospin-$\frac{3}{2}$ transition operator [26]. Using Eq. (4.18) for the latter, the isospin factors for the planar and the crossed TPE diagram can readily be evaluated. One finds for one Δ isobar in the intermediate state for the planar ($//$) and the crossed (X) graph [28]

$$C_{N\Delta}^{(//)}(I) = 2 + \tfrac{2}{3}\boldsymbol{\tau}_1 \cdot \boldsymbol{\tau}_2, \quad C_{N\Delta}^{(X)}(I) = 2 - \tfrac{2}{3}\boldsymbol{\tau}_1 \cdot \boldsymbol{\tau}_2 \ ,$$

$$(4.19)$$

where I denotes the total isospin of the NN state. For two Δ isobars in the intermediate state one gets for the planar and the crossed graphs

$$C_{\Delta\Delta}^{(//)}(I) = \tfrac{4}{3} - \tfrac{2}{9}\boldsymbol{\tau}_1 \cdot \boldsymbol{\tau}_2, \quad C_{\Delta\Delta}^{(X)}(I) = \tfrac{4}{3} + \tfrac{2}{9}\boldsymbol{\tau}_1 \cdot \boldsymbol{\tau}_2 \ .$$

$$(4.20)$$

For the definition of the Fourier transformations to configuration space, we introduce $\mathbf{Q} = \frac{1}{2}(\mathbf{p} + \mathbf{p}')$ and will occasionally exploit the relation $\mathbf{p} - \mathbf{p}' = \mathbf{k} + \mathbf{k}'$ before doing the Fourier transformations.

In the next section, we calculate the TPE contribution to V_C, V_σ, V_T, and V_{SO}, which refer to the central, the spin-spin, the tensor, and the spin-orbit potential, respectively. In Sec. V, we give the so-called adiabatic contributions (see, e.g., Ref. [29] for the definition). In the adiabatic approximation we expand the energy denominators in the expressions for the planar- and crossed-box diagrams in powers of $1/M_N$ and keep only the leading term, order $\mathcal{O}(1)$. For example,

$$\frac{1}{E_{\mathbf{p}} + \mathcal{E}_{\mathbf{p}-\mathbf{k}} - W + \omega} \approx \frac{1}{\omega + a} \ ,$$

$$(4.21)$$

where $a = M_\Delta - M_N$. In the evaluation of the TMO graphs, we encounter the intermediate-state energy denominator $[\mathcal{E}_{\mathbf{p}-\mathbf{k}} + E_{\mathbf{p}-\mathbf{k}} - W]^{-1}$, the treatment of which is explained in Appendix A. Since the leading term of the TMO graphs is cancelled by the once-iterated OPE term [see Eq. (4.12)], the contribution of the TMO graphs has to be evaluated up to order $\mathcal{O}(1/M)$.

The next-to-leading contributions to Eq. (4.21) are referred to as "nonadiabatic" and will be given in Sec. VI. There we also give the (ω/M_N) contributions due to the pseudovector nature of the $NN\pi$ vertex (4.16). They obviously only contribute in the $N\Delta$ graphs. In Sec. VI we only include the first-order recoil corrections. This means that for the TMO potential we do not include the nonadiabatic contribution, which is order $\mathcal{O}(1/M^2)$. In the following sections we work out the various contributions to the TPEP. To distinguish between the different contributions we employ the notations as listed below

Sec.	Type	$N\Delta$	$\Delta\Delta$
V	Adiabatic	$V_{N\Delta}^{(0)}(\alpha)$	$V_{\Delta\Delta}^{(0)}(\alpha)$
VI A	$(1/M)$ adiabatic	$V_{N\Delta}^{(1)}(\alpha)$	—
VI B	$(1/M)$ nonadiabatic	$V_{N\Delta}^{(2)}(\alpha)$	$V_{\Delta\Delta}^{(2)}(\alpha)$

TABLE I. Momentum operators $O^{(\alpha)}(\mathbf{k}_1, \mathbf{k}_2)$ of the planar (BW$_{//}$ and TMO) and crossed (BW$_X$) graphs for the $N\Delta$ and $\Delta\Delta$ intermediate states.

α	$O_{N\Delta}^{(\alpha)}(\mathbf{k}_1, \mathbf{k}_2)$
BW$_{//}$, TMO	$\frac{2}{3}(\mathbf{k}_1 \cdot \mathbf{k}_2)^2 + \frac{1}{3}(\sigma_1 \cdot \mathbf{k}_1 \times \mathbf{k}_2)(\sigma_2 \cdot \mathbf{k}_1 \times \mathbf{k}_2)$
BW$_X$	$\frac{2}{3}(\mathbf{k}_1 \cdot \mathbf{k}_2)^2 - \frac{1}{3}(\sigma_1 \cdot \mathbf{k}_1 \times \mathbf{k}_2)(\sigma_2 \cdot \mathbf{k}_1 \times \mathbf{k}_2)$

α	$O_{\Delta\Delta}^{(\alpha)}(\mathbf{k}_1, \mathbf{k}_2)$
BW$_{//}$, TMO	$\frac{4}{9}(\mathbf{k}_1 \cdot \mathbf{k}_2)^2 - \frac{1}{9}(\sigma_1 \cdot \mathbf{k}_1 \times \mathbf{k}_2)(\sigma_2 \cdot \mathbf{k}_1 \times \mathbf{k}_2)$
BW$_X$	$\frac{4}{9}(\mathbf{k}_1 \cdot \mathbf{k}_2)^2 + \frac{1}{9}(\sigma_1 \cdot \mathbf{k}_1 \times \mathbf{k}_2)(\sigma_2 \cdot \mathbf{k}_1 \times \mathbf{k}_2)$

Here α refers to the different class of potentials BW$_{//}$, BW$_X$, TMO, and the once-iterated OPE contribution.

V. TWO-PION-EXCHANGE POTENTIAL

A. $N\Delta$ graphs

The parallel BW graph (a) of Fig. 3 corresponds to the expression $K_{//}^{(3a)}$ of Eq. (4.3). The crossed BW graphs

(a)–(c) of Fig. 4 correspond to the expressions K_X of Eqs. (4.6a)–(4.6c). The TMO graphs (a) and (b) of Fig. 5 correspond to the expressions of Eqs. (4.4a) and (4.4b).

The TPEP's from the graphs of Figs. 3, 4, and 5 can be written as [30]

$$V_{N\Delta}^{(0)}(\alpha) = -\, C_{N\Delta}^{(\alpha)}(I) \left(\frac{f_{N\Delta\pi}}{m_\pi}\right)^2 \left(\frac{f_{NN\pi}}{m_\pi}\right)^2$$
$$\times \int\int \frac{d^3k_1 d^3k_2}{(2\pi)^6} \, e^{i(\mathbf{k}_1 + \mathbf{k}_2)\cdot\mathbf{r}} \, F(\mathbf{k}_1^2)F(\mathbf{k}_2^2)$$
$$\times O_{N\Delta}^{(\alpha)}(\mathbf{k}_1, \mathbf{k}_2)D_\alpha^{(1)}(\omega_1, \omega_2)\,, \qquad (5.1)$$

where I denotes the total isospin of the NN channel ($I = 0, 1$) and α refers to the different class of graphs BW$_{//}$, BW$_X$, and TMO. The isospin factor $C_{N\Delta}$ is given in Eq. (4.19). The operator $O^{(\alpha)}(\mathbf{k}_1, \mathbf{k}_2)$ contains the vertex operators, given in Eqs. (4.16) and (4.17), and the explicit expressions for each case α are given in Table I. In all expressions we have made use of the symmetry $\mathbf{k}_1 \leftrightarrow \mathbf{k}_2$ to discard the antisymmetric terms. From Table I we can define factors $\gamma_{1,i}$, which are the rational numbers in front of the momentum operators. These enable us to write the expressions for the potentials in a

TABLE II. Adiabatic approximation of the energy denominators $D_\alpha^{(1)}$ for $N\Delta$ and $D_\alpha^{(2)}$ for $\Delta\Delta$ intermediate states. Here $\beta_1 = \mathbf{k}_1 \cdot \mathbf{k}_2/\overline{M}$ and $\beta_2 = \mathbf{k}_1 \cdot \mathbf{k}_2/M_\Delta$.

α	$D_\alpha^{(1)}(\omega_1, \omega_2)$
BW$_{//}$	$\dfrac{1}{2\omega_1\omega_2}\left[\dfrac{1}{(\omega_1 + a)\omega_2} + \dfrac{1}{\omega_1(\omega_2 + a)}\right]\dfrac{1}{(\omega_1 + \omega_2)}$
BW$_X$	$\dfrac{1}{2\omega_1\omega_2}\left\{\left[\dfrac{1}{(\omega_1 + a)\omega_1} + \dfrac{1}{(\omega_2 + a)\omega_2}\right]\left(\dfrac{1}{\omega_1 + \omega_2} + \dfrac{1}{\omega_1 + \omega_2 + a}\right) + \left[\dfrac{1}{(\omega_1 + a)(\omega_2 + a)} + \dfrac{1}{\omega_1\omega_2}\right]\dfrac{1}{\omega_1 + \omega_2 + a}\right\}$
TMO	$\dfrac{1}{4\omega_1\omega_2}\left[\dfrac{1}{(\omega_1 + a)\omega_2}\left(\dfrac{1}{\omega_1 + a} + \dfrac{1}{\omega_2}\right) + \dfrac{1}{\omega_1(\omega_2 + a)}\left(\dfrac{1}{\omega_1} + \dfrac{1}{\omega_2 + a}\right) + \dfrac{1}{\omega_1\omega_2}\left(\dfrac{1}{\omega_1} + \dfrac{1}{\omega_2}\right)\right.$ $\left. + \dfrac{1}{(\omega_1 + a)(\omega_2 + a)}\left(\dfrac{1}{\omega_1 + a} + \dfrac{1}{\omega_2 + a}\right)\right]\dfrac{\beta_1}{a - \beta_1}$
Born	$\dfrac{1}{2\omega_1\omega_2}\left[\dfrac{1}{(\omega_1 + a)\omega_2} + \dfrac{1}{\omega_1(\omega_2 + a)} + \dfrac{1}{(\omega_1 + a)(\omega_2 + a)} + \dfrac{1}{\omega_1\omega_2}\right]\dfrac{1}{a - \beta_1}$

α	$D_\alpha^{(2)}(\omega_1, \omega_2)$
BW$_{//}$	$\dfrac{1}{2\omega_1\omega_2}\left[\dfrac{1}{(\omega_1 + a)(\omega_2 + a)}\,\dfrac{1}{(\omega_1 + \omega_2)}\right]$
BW$_X$	$\dfrac{1}{4\omega_1\omega_2}\left[\left(\dfrac{1}{(\omega_1 + a)^2} + \dfrac{1}{(\omega_2 + a)^2}\right)\dfrac{1}{(\omega_1 + \omega_2)} + \left(\dfrac{1}{(\omega_1 + a)^2} + \dfrac{1}{(\omega_2 + a)^2} + \dfrac{2}{(\omega_1 + a)(\omega_2 + a)}\right)\dfrac{1}{(\omega_1 + \omega_2 + 2a)}\right]$
TMO	$\dfrac{1}{4\omega_1\omega_2}\left[\dfrac{1}{(\omega_1 + a)^2(\omega_2 + a)} + \dfrac{1}{(\omega_1 + a)(\omega_2 + a)^2}\right]\dfrac{\beta_2}{2a - \beta_2}$
Born	$\dfrac{1}{\omega_1\omega_2}\left[\dfrac{1}{(\omega_1 + a)(\omega_2 + a)}\right]\dfrac{1}{2a - \beta_2}$

concise form. To be explicit, we have

$$\gamma_{1,C}^{(//)} = \tfrac{2}{3}, \quad \gamma_{1,\sigma}^{(//)} = \gamma_{1,T}^{(//)} = \tfrac{1}{3},$$

(5.2)

$$\gamma_{1,C}^{(X)} = \tfrac{2}{3}, \quad \gamma_{1,\sigma}^{(X)} = \gamma_{1,T}^{(X)} = -\tfrac{1}{3},$$

where C, σ, T refer to the central, spin-spin, and tensor parts of the potential.

The energy denominators $D_\alpha^{(1)}$ of the TPE process are calculated in the adiabatic approximation, i.e., $E(\mathbf{p}) \approx M_N$ and $\mathcal{E}(\mathbf{p}) \approx M_\Delta$. The appropriate expressions in terms of $\omega_i = \omega(\mathbf{k}_i)$, including the contributions from *all* graphs, are given in the upper half of Table II. The latter also contains the $1/\sqrt{2\omega}$ factors from the pion field at each vertex. Note that for the TMO graphs we have expanded up to order $\mathcal{O}(1/M)$ and already subtracted the once-iterated OPE contribution, in accordance with Eq. (4.12). The intermediate-state energy denominator $\mathcal{E}_{\mathbf{p}-\mathbf{k}_1} + E_{\mathbf{p}-\mathbf{k}_1} - W$ is approximated by $(a - \beta_1)$ with $\beta_1 = \mathbf{k}_1 \cdot \mathbf{k}_2/\overline{M}$ and $\overline{M} = (M_\Delta + M_N)/2$ (see also Sec. VI B).

The evaluation of the momentum integrations is readily performed using the formulas given in Appendix B.

Since in Appendix B it is shown that the separation of the $\mathbf{k}_1$ and $\mathbf{k}_2$ variables can be achieved in all cases, we can use the same procedure as given in Ref. [1]. We write

$$e^{i(\mathbf{k}_1+\mathbf{k}_2)\cdot\mathbf{r}} = \lim_{\mathbf{r}_1,\mathbf{r}_2\to\mathbf{r}} e^{i\mathbf{k}_1\cdot\mathbf{r}_1} e^{i\mathbf{k}_2\cdot\mathbf{r}_2},$$

(5.3)

and take the limit operation before the momentum integrations. Next, we replace all momenta occurring in the numerator by $\boldsymbol{\nabla}_1$ and $\boldsymbol{\nabla}_2$ operations, which are the $\boldsymbol{\nabla}$ operations with respect to $\mathbf{r}_1$ and $\mathbf{r}_2$, respectively, and take these in front of the momentum integrations. After the momentum integrations we perform the differentiations and take the limit. The structure of the potentials which will appear in the course of this calculation are explained in Appendix C. There we introduce the $\otimes$ operation, which allows us to write the expressions for the potentials in a succinct form. The results we obtain are

(i) BW-parallel graphs. Application of Eqs. (B9) and (B11), together with the definitions (C6) and (C7) leads to the expressions for the potentials given in this item. The other expressions of this and the following sections can be derived similarly. We find

$$V_{N\Delta,i}^{(0)}(\mathrm{BW}_{//}) = -\, C_{N\Delta}^{(//)}(I) \left(\frac{f_{N\Delta\pi}}{m_\pi}\right)^2 \left(\frac{f_{NN\pi}}{m_\pi}\right)^2 \gamma_{1,i}^{(//)}$$
$$\times \left[\frac{a}{2}(G_{2,1}\otimes G_{2,1})_i(r) - \frac{1}{a}(G_{1,1}\otimes G_{1,1})_i(r) + \frac{2}{\pi}\int_0^\infty \frac{d\lambda}{a^2+\lambda^2}(F\otimes F)_i(\lambda,r)\right],$$

(5.4)

where $i = C, \sigma, T$, and

$$F(\lambda,r) = I_2(\sqrt{m_\pi^2 + \lambda^2}, r)\exp\left(-\lambda^2/\Lambda^2\right).$$

The functions $I_2(m_\pi, r), G_{1,1}(a, r)$, and $G_{2,1}(a, r)$ are defined in Eqs. (B4), (B14), and (B16) of Appendix B, respectively.

(ii) BW-crossed graphs.

$$V_{N\Delta,i}^{(0)}(\mathrm{BW}_X) = -\, C_{N\Delta}^{(X)}(I) \left(\frac{f_{N\Delta\pi}}{m_\pi}\right)^2 \left(\frac{f_{NN\pi}}{m_\pi}\right)^2 \gamma_{1,i}^{(X)}$$
$$\times \left[-a(G_{2,1}\otimes G_{2,1})_i(r) + \frac{1}{a}(G_{1,1}\otimes G_{1,1})_i(r) + 2(I_2\otimes G_{2,1})_i(r) - \frac{2}{\pi}\int_0^\infty \frac{d\lambda}{a^2+\lambda^2}(F\otimes F)_i(\lambda,r)\right].$$

(5.5)

(iii) TMO graphs.

$$V_{N\Delta,i}^{(0)}(\mathrm{TMO})$$

$$= -\, C_{N\Delta}^{(//)}(I) \left(\frac{f_{N\Delta\pi}}{m_\pi}\right)^2 \left(\frac{f_{NN\pi}}{m_\pi}\right)^2 \gamma_{1,i}^{(//)}$$
$$\times \Bigg\{ a\int_0^\infty dz\, e^{-z(a-\frac{1}{2}T_{\mathrm{lab}})}\tfrac{1}{2}\left[(I_3\otimes G_{1,1})_i(z;r) + (I_2\otimes G_{1,2})_i(z;r) + (G_{1,1}\otimes G_{1,2})_i(z;r) + (I_2\otimes I_3)_i(z;r)\right]$$
$$-\tfrac{1}{2}\left[(I_3\otimes G_{1,1})_i(r) + (I_2\otimes G_{1,2})_i(r) + (G_{1,1}\otimes G_{1,2})_i(r) + (I_2\otimes I_3)_i(r)\right]\Bigg\},$$

(5.6)

where the separation into the two contributions between square brackets is explained in Appendix A.

B. $\Delta\Delta$ graphs

The parallel BW graph of Fig. 6 corresponds to the expression $K_{//}^{(3a)}$ of Eq. (4.3), substituting $E_{\mathbf{p}-\mathbf{k}} \to \mathcal{E}_{\mathbf{p}-\mathbf{k}}$. The TMO graphs in Fig. 8 correspond to the expressions in Eqs. (4.4a) and (4.4b) using the same substitution. The crossed BW graphs of Fig. 7 correspond to the expressions in Eqs. (4.6a)–(4.6c), substituting $E_{\mathbf{p}'+\mathbf{k}} \to \mathcal{E}_{\mathbf{p}'+\mathbf{k}}$.

The TPEP's from these graphs with two Δ isobars in the intermediate states can be evaluated completely analogous to the one-Δ graphs. The result can be written as

$$V_{\Delta\Delta}^{(0)}(\alpha) = -C_{\Delta\Delta}^{(\alpha)}(I) \left(\frac{f_{N\Delta\pi}}{m_\pi}\right)^4 \int\int \frac{d^3k_1 d^3k_2}{(2\pi)^6} e^{i(\mathbf{k}_1+\mathbf{k}_2)\cdot\mathbf{r}} O_{\Delta\Delta}^{(\alpha)}(\mathbf{k}_1,\mathbf{k}_2) F(\mathbf{k}_1^2) F(\mathbf{k}_2^2) D_\alpha^{(2)}(\omega_1,\omega_2) , \qquad (5.7)$$

where α again refers to the different class of graphs $\mathrm{BW}_{//}$, BW_X, and TMO. The isospin factors $C_{\Delta\Delta}$ are given in Eq. (4.20). For the different cases α we have given the explicit expressions for $O_{\Delta\Delta}(\mathbf{k}_1,\mathbf{k}_2)$ in Table I. Similarly as for the $N\Delta$ case, we define factors $\gamma_{2,i}$ which are now found to be

$$\gamma_{2,C}^{(//)} = \tfrac{4}{9}, \quad \gamma_{2,\sigma}^{(//)} = \gamma_{2,T}^{(//)} = -\tfrac{1}{9},$$

$$\gamma_{2,C}^{(X)} = \tfrac{4}{9}, \quad \gamma_{2,\sigma}^{(X)} = \gamma_{2,T}^{(X)} = \tfrac{1}{9} . \qquad (5.8)$$

The energy denominators $D_\alpha^{(2)}$ are given in the lower half of Table II, where again the adiabatic approximation is made. In the TMO graphs the intermediate-state energy denominator $\mathcal{E}_{\mathbf{p}-\mathbf{k}_1}+\mathcal{E}_{\mathbf{p}-\mathbf{k}_1}-W$ is approximated by $(2a-\beta_2)$ with now $\beta_2 = \mathbf{k}_1\cdot\mathbf{k}_2/M_\Delta$. In Table II, the expression in square brackets for $D_X^{(2)}$ can be written as

$$D_X^{(2)} = -2\frac{d}{da}\left[\frac{a}{(\omega_1+a)(\omega_2+a)(\omega_1+\omega_2)} + \frac{1}{(\omega_1+a)(\omega_2+a)} \right] . \qquad (5.9)$$

In this form, the Fourier transformation to configuration space can be carried through immediately using the results given in Appendix B.

The momentum integrations can be carried out similarly to those in the foregoing section. We find the following.
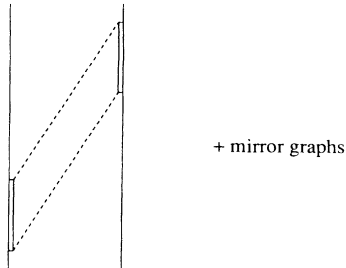
(i) BW-parallel graphs.

$$V_{\Delta\Delta,i}^{(0)}(\mathrm{BW}_{//}) = -C_{\Delta\Delta}^{(//)}(I) \left(\frac{f_{N\Delta\pi}}{m_\pi}\right)^4 \gamma_{2,i}^{(//)}$$

$$\times \left\{ \frac{1}{\pi}\int_0^\infty \frac{d\lambda}{a^2+\lambda^2}(F\otimes F)_i(\lambda,r) \right.$$

$$\left. -\frac{1}{2a}(G_{1,1}\otimes G_{1,1})_i(r) \right\} . \qquad (5.10)$$

(ii) BW-crossed graphs.

$$V_{\Delta\Delta,i}^{(0)}(\mathrm{BW}_X) = -C_{\Delta\Delta}^{(X)}(I) \left(\frac{f_{N\Delta\pi}}{m_\pi}\right)^4 \gamma_{2,i}^{(X)}$$

$$\times \frac{1}{\pi}\int_0^\infty d\lambda \frac{a^2-\lambda^2}{(a^2+\lambda^2)^2}(F\otimes F)_i(r). \qquad (5.11)$$

+ mirror graphs

FIG. 6.   Planar BW two-pion-exchange potential graphs with two Δ_{33} isobars in the intermediate state.

+ mirror graphs
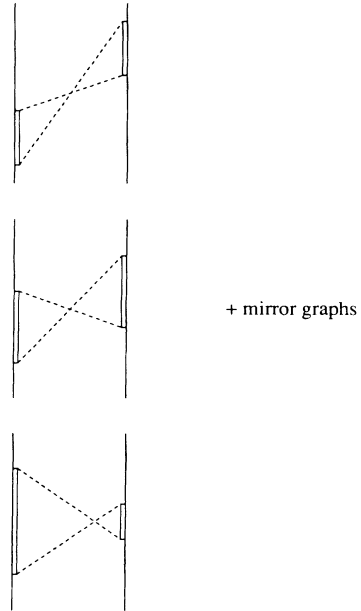
FIG. 7.   Crossed BW two-pion-exchange potential graphs with two Δ_{33} isobars in the intermediate state.

(iii) TMO graphs.

$$V_{\Delta\Delta,i}^{(0)}(\text{TMO}) = -C_{\Delta\Delta}^{(//)}(I)\left(\frac{f_{N\Delta\pi}}{m_\pi}\right)^4 \gamma_{2,i}^{(//)}\left\{a\int_0^\infty dz\, e^{-z(2a-\frac{1}{2}T_{\text{lab}})}(G_{1,1}\otimes G_{1,2})_i(z;r) - \tfrac{1}{2}(G_{1,1}\otimes G_{1,2})_i(r)\right\}. \quad (5.12)$$

C. Iterated one-pion exchange

Our definition of the TMO potential, Eq. (4.12), explicitly includes the subtraction of the once-iterated OPE. However, in case of a single-channel Lippmann-Schwinger or Schrödinger calculation for the NN channel, one should include only the pure TMO diagrams (next to the BW diagrams, of course). This can simply be achieved by adding to the TMO potentials of Eqs. (5.6) and (5.12) the second-order Born approximation to the interaction kernels. These are given by the following.

(i) $N\Delta$ graphs. The $N\Delta$ graph of Fig. 9 gives the kernel

$$K_{\text{Born}}^{(4)}(r) = -C_{N\Delta}^{(//)}(I)\left(\frac{f_{N\Delta\pi}}{m_\pi}\right)^2\left(\frac{f_{NN\pi}}{m_\pi}\right)^2$$

$$\times\int\int\frac{d^3k_1 d^3k_2}{(2\pi)^6}e^{i(\mathbf{k}_1+\mathbf{k}_2)\cdot\mathbf{r}}F(\mathbf{k}_1^2)\,F(\mathbf{k}_2^2)$$

$$\times O_{N\Delta}^{(//)}(\mathbf{k}_1,\mathbf{k}_2)D_{\text{Born}}^{(1)}(\omega_1,\omega_2)\,, \quad (5.13)$$

where $D_{\text{Born}}^{(1)}$ can be found in Table II. Our treatment of the intermediate-state energy denominator $(a-\beta_1)$ is explained in Appendix A. The resulting potential reads

$$V_{N\Delta,i}^{(4)}(\text{Born}) = -C_{N\Delta}^{(//)}(I)\left(\frac{f_{N\Delta\pi}}{m_\pi}\right)^2\left(\frac{f_{NN\pi}}{m_\pi}\right)^2\gamma_{1,i}^{(//)}$$

$$\times\tfrac{1}{2}\int_0^\infty dz\, e^{-z(a-\frac{1}{2}T_{\text{lab}})}[2(I_2\otimes G_{1,1})_i(z;r) + (G_{1,1}\otimes G_{1,1})_i(z;r) + (I_2\otimes I_2)_i(z;r)]\,. \quad (5.14)$$

(ii) $\Delta\Delta$ graphs. The $\Delta\Delta$ graph of Fig. 9 gives the kernel

$$K_{\text{Born}}^{(4)}(r) = -C_{\Delta\Delta}^{(//)}(I)\left(\frac{f_{N\Delta\pi}}{m_\pi}\right)^4\int\int\frac{d^3k_1 d^3k_2}{(2\pi)^6}e^{i(\mathbf{k}_1+\mathbf{k}_2)\cdot\mathbf{r}}F(\mathbf{k}_1^2)\,F(\mathbf{k}_2^2)O_{\Delta\Delta}^{(//)}(\mathbf{k}_1,\mathbf{k}_2)D_{\text{Born}}^{(2)}(\omega_1,\omega_2)\,, \quad (5.15)$$

where $D_{\text{Born}}^{(2)}$ is given in Table II. The corresponding potential reads

$$V_{\Delta\Delta,i}^{(4)}(\text{Born}) = -C_{\Delta\Delta}^{(//)}(I)\left(\frac{f_{N\Delta\pi}}{m_\pi}\right)^4 \gamma_{2,i}^{(//)}\int_0^\infty dz\, e^{-z(2a-\frac{1}{2}T_{\text{lab}})}(G_{1,1}\otimes G_{1,1})_i(z;r)\,. \quad (5.16)$$

So, for an $(NN, N\Delta) \to (NN, N\Delta)$ coupled-channel calculation the potential of Eq. (5.16) should be added to the TMO potential of Eq. (5.12) in order to compensate for the subtraction of the iterated OPE with two Δ isobars in the intermediate states. For a single-channel NN calculation one has to add the potentials of both
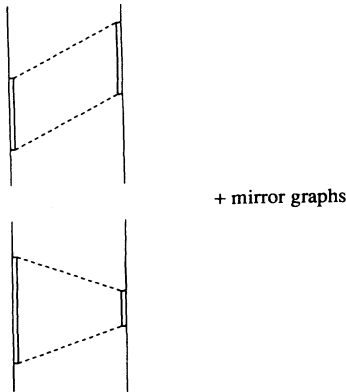
Eqs. (5.14) and (5.16) to the TMO potentials of Eqs. (5.6) and (5.12), respectively.

VI. 1/M CORRECTIONS

A. Corrections from pseudovector vertex

The adiabatic $(1/M)$ corrections originate from the ω/M_N terms of the $NN\pi$ vertex of Eq. (4.16). These

+ mirror graphs

FIG. 8. TMO two-pion-exchange potential graphs with two Δ_{33} isobars in the intermediate state.
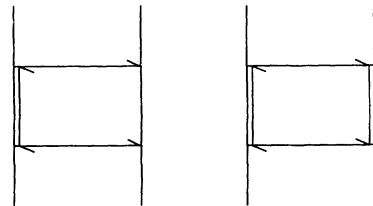
FIG. 9. Second-order potential scattering diagrams with (a) one or (b) two Δ_{33} isobars in the intermediate state.

TABLE III.   Momentum operators $O'(\mathbf{k}_1, \mathbf{k}_2)$ for the adiabatic (m_π/M) corrections of the $\mathrm{BW}_{//}$, the BW_X, and the Born graphs for $N\Delta$ intermediate states.

α	$O_{N\Delta}^{\prime(\alpha)}(\omega_1, \mathbf{k}_1; \omega_2, \mathbf{k}_2)$
$\mathrm{BW}_{//}$	$\frac{2}{3}\left[(\mathbf{k}_1 \cdot \mathbf{k}_2)\left(\omega_1\mathbf{k}_2^2 - \omega_2\mathbf{k}_1^2\right) + i(\mathbf{k}_1 \cdot \mathbf{k}_2)(\omega_1\mathbf{k}_2 - \omega_2\mathbf{k}_1) \times \mathbf{Q} \cdot (\sigma_1 + \sigma_2) + \frac{i}{2}(\sigma_1 + \sigma_2) \cdot \mathbf{k}_1 \times \mathbf{k}_2 \, (\omega_1\mathbf{k}_2 + \omega_2\mathbf{k}_1) \cdot \mathbf{Q}\right]$
$\mathrm{BW}_{X,a}$	$\frac{2}{3}\left[-(\mathbf{k}_1 \cdot \mathbf{k}_2)\left(\omega_1\mathbf{k}_2^2 - \omega_2\mathbf{k}_1^2\right) - i(\mathbf{k}_1 \cdot \mathbf{k}_2)(\omega_1\mathbf{k}_2 - \omega_2\mathbf{k}_1) \times \mathbf{Q} \cdot (\sigma_1 + \sigma_2) + \frac{i}{2}(\sigma_1 + \sigma_2) \cdot \mathbf{k}_1 \times \mathbf{k}_2 \, (\omega_1\mathbf{k}_2 + \omega_2\mathbf{k}_1) \cdot \mathbf{Q}\right]$
$\mathrm{BW}_{X,b}$	$\frac{2}{3}\left[-(\mathbf{k}_1 \cdot \mathbf{k}_2)\left(\omega_1\mathbf{k}_2^2 + \omega_2\mathbf{k}_1^2\right) - i(\mathbf{k}_1 \cdot \mathbf{k}_2)(\omega_1\mathbf{k}_2 + \omega_2\mathbf{k}_1) \times \mathbf{Q} \cdot (\sigma_1 + \sigma_2) + \frac{i}{2}(\sigma_1 + \sigma_2) \cdot \mathbf{k}_1 \times \mathbf{k}_2 \, (\omega_1\mathbf{k}_2 - \omega_2\mathbf{k}_1) \cdot \mathbf{Q}\right]$
Born, a	$\frac{2}{3}\left[(\mathbf{k}_1 \cdot \mathbf{k}_2)\left(\omega_1\mathbf{k}_2^2 - \omega_2\mathbf{k}_1^2\right) + i(\mathbf{k}_1 \cdot \mathbf{k}_2)(\omega_1\mathbf{k}_2 - \omega_2\mathbf{k}_1) \times \mathbf{Q} \cdot (\sigma_1 + \sigma_2) + \frac{i}{2}(\sigma_1 + \sigma_2) \cdot \mathbf{k}_1 \times \mathbf{k}_2 \, (\omega_1\mathbf{k}_2 + \omega_2\mathbf{k}_1) \cdot \mathbf{Q}\right]$
Born, b	$\frac{2}{3}\left[(\mathbf{k}_1 \cdot \mathbf{k}_2)\left(\omega_1\mathbf{k}_2^2 + \omega_2\mathbf{k}_1^2\right) + i(\mathbf{k}_1 \cdot \mathbf{k}_2)(\omega_1\mathbf{k}_2 + \omega_2\mathbf{k}_1) \times \mathbf{Q} \cdot (\sigma_1 + \sigma_2) + \frac{i}{2}(\sigma_1 + \sigma_2) \cdot \mathbf{k}_1 \times \mathbf{k}_2 \, (\omega_1\mathbf{k}_2 - \omega_2\mathbf{k}_1) \cdot \mathbf{Q}\right]$

terms are typical for the pseudovector coupling of the pseudoscalars and in particular will give a spin-orbit potential $V_{N\Delta,SO}^{(1)}(\alpha) \, \mathbf{L} \cdot \mathbf{S}$. The different contributions can be written as

$$V_{N\Delta}^{(1)}(\alpha) = -\, C_{N\Delta}^{(\alpha)}(I)\left(\frac{f_{N\Delta\pi}}{m_\pi}\right)^2\left(\frac{f_{NN\pi}}{m_\pi}\right)^2 \frac{1}{M_N}$$
$$\times \int\int \frac{d^3k_1 d^3k_2}{(2\pi)^6} e^{i(\mathbf{k}_1+\mathbf{k}_2)\cdot\mathbf{r}} F(\mathbf{k}_1^2)\, F(\mathbf{k}_2^2)$$
$$\times O_{N\Delta}^{(\alpha)\prime}(\omega_1, \mathbf{k}_1; \omega_2, \mathbf{k}_2) D_\alpha'(\omega_1, \omega_2)\, .$$
(6.1)

For the different cases α, the explicit expressions for $O_{N\Delta}'(\mathbf{k}_1, \mathbf{k}_2)$ and D_α' are given in Tables III and IV, respectively. There, $\mathrm{BW}_{X,a}$ refers to graphs (a) and (a')

TABLE IV.   Adiabatic approximation of the energy denominators D_α' for contributions from (m_π/M) corrections of the $NN\pi$ vertex for the $\mathrm{BW}_{//}$, the BW_X, and the Born graphs for $N\Delta$ intermediate states; $\beta_1 = \mathbf{k}_1 \cdot \mathbf{k}_2/M$.

α	$D_\alpha'(\omega_1, \omega_2)$
$\mathrm{BW}_{//}$	$\frac{1}{4\omega_1\omega_2}\left[\frac{1}{(\omega_1 + a)\omega_2} - \frac{1}{\omega_1(\omega_2 + a)}\right]\frac{1}{(\omega_1 + \omega_2)}$
$\mathrm{BW}_{X,a}$	$\frac{1}{4\omega_1\omega_2}\left[\frac{1}{(\omega_1 + a)\omega_1} - \frac{1}{(\omega_2 + a)\omega_2}\right]\frac{1}{(\omega_1 + \omega_2)}$
$\mathrm{BW}_{X,b}$	$\frac{1}{4\omega_1^2\omega_2^2}\left[\frac{1}{(\omega_1 + a)} + \frac{1}{(\omega_2 + a)} - \frac{a}{(\omega_1 + a)(\omega_2 + a)}\right]$
Born, a	$\frac{1}{4\omega_1\omega_2}\left[\frac{1}{(\omega_1 + a)\omega_2} - \frac{1}{\omega_1(\omega_2 + a)}\right]\frac{1}{a - \beta_1}$
Born, b	$\frac{1}{4\omega_1\omega_2}\left[\frac{1}{(\omega_1 + a)(\omega_2 + a)} - \frac{1}{\omega_1\omega_2}\right]\frac{1}{a - \beta_1}$

of Fig. 4, and $\mathrm{BW}_{X,b}$ refers to graphs (b), (b'), (c), and (c'). Note that the Born and TMO graphs give rise to the same pseudovector vertex corrections, so they do not contribute in what we refer to as the TMO potential, which includes the Born subtraction. Again, the isospin factors $C_{N\Delta}(I)$ are those of Eq. (4.19).

In order to be able to evaluate the integrals in an easy way, we define for the planar graphs

$$\widetilde{O}_{//}^{\pm}(\mathbf{k}_1, \mathbf{k}_2) = \pm\frac{1}{3}\left[\, (\mathbf{k}_1 \cdot \mathbf{k}_2)\,(\mathbf{k}_1^2 \pm \mathbf{k}_2^2)\right.$$
$$+2i(\mathbf{k}_1 \cdot \mathbf{k}_2)\,(\mathbf{k}_1 \pm \mathbf{k}_2) \times \mathbf{Q} \cdot \mathbf{S}$$
$$\left. -i(\mathbf{k}_1 \times \mathbf{k}_2) \cdot \mathbf{S}\,(\mathbf{k}_1 \mp \mathbf{k}_2) \cdot \mathbf{Q}\right]\, , \quad (6.2)$$

and for the crossed graphs

$$\widetilde{O}_X^{\pm}(\mathbf{k}_1, \mathbf{k}_2) = \pm\frac{1}{3}[\, -(\mathbf{k}_1 \cdot \mathbf{k}_2)\,(\mathbf{k}_1^2 \pm \mathbf{k}_2^2)$$
$$-2i(\mathbf{k}_1 \cdot \mathbf{k}_2)\,(\mathbf{k}_1 \pm \mathbf{k}_2) \times \mathbf{Q} \cdot \mathbf{S}$$
$$-i(\mathbf{k}_1 \times \mathbf{k}_2) \cdot \mathbf{S}\,(\mathbf{k}_1 \mp \mathbf{k}_2) \cdot \mathbf{Q}]\, . \quad (6.3)$$

The operators $O_{N\Delta}^{(\alpha)\prime}$ of Table III can then be written successively as

$$(\omega_1 - \omega_2)\widetilde{O}_{//}^{+}(\mathbf{k}_1, \mathbf{k}_2) + (\omega_1 + \omega_2)\widetilde{O}_{//}^{-}(\mathbf{k}_1, \mathbf{k}_2)\, ,$$
$$(\omega_1 - \omega_2)\widetilde{O}_X^{+}(\mathbf{k}_1, \mathbf{k}_2) + (\omega_1 + \omega_2)\widetilde{O}_X^{-}(\mathbf{k}_1, \mathbf{k}_2)\, ,$$
$$(\omega_1 + \omega_2)\widetilde{O}_X^{+}(\mathbf{k}_1, \mathbf{k}_2) + (\omega_1 - \omega_2)\widetilde{O}_X^{-}(\mathbf{k}_1, \mathbf{k}_2)\, , \quad (6.4)$$
$$(\omega_1 - \omega_2)\widetilde{O}_{//}^{+}(\mathbf{k}_1, \mathbf{k}_2) + (\omega_1 + \omega_2)\widetilde{O}_{//}^{-}(\mathbf{k}_1, \mathbf{k}_2)\, ,$$
$$(\omega_1 + \omega_2)\widetilde{O}_{//}^{+}(\mathbf{k}_1, \mathbf{k}_2) + (\omega_1 - \omega_2)\widetilde{O}_{//}^{-}(\mathbf{k}_1, \mathbf{k}_2)\, .$$

The potentials (6.1) can now be written in general as

$$V^{(1)}_{N\Delta}(\alpha) = -C^{(\alpha)}_{N\Delta}(I)\left(\frac{f_{N\Delta\pi}}{m_\pi}\right)^2\left(\frac{f_{NN\pi}}{m_\pi}\right)^2\frac{1}{M_N}\sum_{s=+,-}\lim_{r_1\to r_2}\widetilde{O}^s_\alpha(-i\nabla_1,-i\nabla_2)A^s_\alpha(r_1,r_2)\ ,\tag{6.5}$$

where the $A^\pm_\alpha(r_1,r_2)$ denote the Fourier transforms of the energy-denominator combinations that occur. They read

$$A^-_{\mathrm{BW}_{//}}(r_1,r_2)=\frac{a}{4}[G_{1,1}(r_1)G_{2,1}(r_2)-G_{2,1}(r_1)G_{1,1}(r_2)]\ ,$$

$$A^+_{\mathrm{BW}_{//}}(r_1,r_2)=\frac{a}{4}[G_{1,1}(r_1)G_{2,1}(r_2)+G_{2,1}(r_1)G_{1,1}(r_2)-4H_{1,1}(r_1,r_2)]\ .\tag{6.6}$$

$$A^-_{\mathrm{BW}_X}(r_1,r_2)=0\ ,$$

$$A^+_{\mathrm{BW}_X}(r_1,r_2)=G_{1,1}(r_1)G_{1,1}(r_2)+aH_{1,1}(r_1,r_2)\ .\tag{6.7}$$

$$A^-_{\mathrm{Born}}(r_1,r_2)=-\frac{a^2}{4}\int_0^\infty dze^{-z(a-\frac{1}{2}T_{\mathrm{lab}})}[G_{1,1}(r_1)G_{2,1}(r_2)-G_{2,1}(r_1)G_{1,1}(r_2)]\ ,$$

$$A^+_{\mathrm{Born}}(r_1,r_2)=-a\int_0^\infty dze^{-z(a-\frac{1}{2}T_{\mathrm{lab}})}\left\{G_{1,1}(r_1)G_{1,1}(r_2)+\frac{a}{4}[G_{1,1}(r_1)G_{2,1}(r_2)+G_{2,1}(r_1)G_{1,1}(r_2)]\right\}\ .\tag{6.8}$$

The functions $G_{1,1}(r)$, $G_{2,1}(r)$, and $H_{1,1}(r_1,r_2)$ are defined in Eqs. (B14) and (B16) of Appendix B, respectively.

In Appendix C, we introduce various $\oslash$ operations, working on functions $F(r)$ and $G(r)$. It will be convenient to define the central and spin-orbit combinations

$$(F\oslash G)_C=(F\oslash G)^+_C-(F\oslash G)^-_C\ ,$$
$$(F\oslash G)_{SO_{//}}=-2(F\oslash G)^+_1+(F\oslash G)^+_2+2(F\oslash G)^-_1-(F\oslash G)^-_2\ ,$$
$$(F\oslash G)_{SO_X}=-2(F\oslash G)^+_1-(F\oslash G)^+_2+2(F\oslash G)^-_1+(F\oslash G)^-_2\ .\tag{6.9}$$

The explicit results can then be written as follows. *(i) BW-parallel graphs.*

$$V^{(1)}_{N\Delta,i}(\mathrm{BW}_{//})=-C^{(//)}_{N\Delta}(I)\left(\frac{f_{N\Delta\pi}}{m_\pi}\right)^2\left(\frac{f_{NN\pi}}{m_\pi}\right)^2\frac{a}{3M_N}$$
$$\times\left[\frac{1}{2}(G_{1,1}\oslash G_{2,1})_i(r)+\frac{1}{a}(G_{1,1}\oslash G_{1,1})_i(r)-\frac{2}{\pi}\int_0^\infty\frac{d\lambda}{a^2+\lambda^2}(F\oslash F)_i(\lambda,r)\right]\ ,\tag{6.10}$$

where $i=C,SO_{//}$. *(ii) BW-crossed graphs.*

$$V^{(1)}_{N\Delta,i}(\mathrm{BW}_X)=-C^{(X)}_{N\Delta}(I)\left(\frac{f_{N\Delta\pi}}{m_\pi}\right)^2\left(\frac{f_{NN\pi}}{m_\pi}\right)^2\frac{a}{3M_N}\left[-\frac{2}{\pi}\int_0^\infty\frac{d\lambda}{a^2+\lambda^2}(F\oslash F)_i(\lambda,r)\right]\ ,\tag{6.11}$$

where $i=C,SO_X$. *(iii) Born graphs.*

$$V^{(1)}_{N\Delta,i}(\mathrm{Born})=+C^{(//)}_{N\Delta}(I)\left(\frac{f_{N\Delta\pi}}{m_\pi}\right)^2\left(\frac{f_{NN\pi}}{m_\pi}\right)^2\frac{a}{3M_N}$$
$$\times\int_0^\infty dze^{-z(a-\frac{1}{2}T_{\mathrm{lab}})}\left[\frac{a}{2}(G_{1,1}\oslash G_{2,1})_i(z;r)+(G_{1,1}\oslash G_{1,1})_i(z;r)\right]\ ,\tag{6.12}$$

where $i=C,SO_{//}$.

B. Nonadiabatic corrections

In the following we will use an average-mass approximation for the $N\Delta$ graphs. With $\overline{M}=(M_\Delta+M_N)/2$, we have $M_N=\overline{M}-a/2$ and $M_\Delta=\overline{M}+a/2$. Therefore

$$\frac{1}{M_N}\approx\frac{1}{\overline{M}}\left(1+\frac{a}{4\overline{M}}\right)\approx\frac{1}{\overline{M}}\ ,$$
$$\frac{1}{M_\Delta}\approx\frac{1}{\overline{M}}\left(1-\frac{a}{4\overline{M}}\right)\approx\frac{1}{\overline{M}}\ .$$

In order to obtain all contributions to the potentials up to order $(m_\pi/\overline{M})$, we expand the three energy denominators in the expressions for the planar- and crossed-box diagrams (see Sec. V) in $1/\overline{M}$. Then, we get, for example,

$$\frac{1}{E_{\mathbf{p}} + \mathcal{E}_{\mathbf{p-k}} - W + \omega}$$

$$= \frac{1}{\omega + a}\left[1 - \frac{-2\mathbf{p}\cdot\mathbf{k} + \mathbf{k}^2}{2\overline{M}(\omega + a)} + \cdots\right] , \quad (6.13)$$

where we neglected the purely off-energy-shell contribution $\mathbf{p}^2 - \mathbf{p}_i^2$, with $\mathbf{p}_i$ the initial-state momentum. This also implies, for example, that

$$\begin{aligned}
-2\mathbf{p}\cdot\mathbf{k}_1 + \mathbf{k}_1^2 &\approx -\mathbf{Q}\cdot(\mathbf{k}_1 - \mathbf{k}_2) - \mathbf{k}_1\cdot\mathbf{k}_2, \\
2\mathbf{p}'\cdot\mathbf{k}_1 + \mathbf{k}_1^2 &\approx +\mathbf{Q}\cdot(\mathbf{k}_1 - \mathbf{k}_2) - \mathbf{k}_1\cdot\mathbf{k}_2, \quad (6.14) \\
-2\mathbf{p}\cdot\mathbf{k}_2 + \mathbf{k}_2^2 &\approx +\mathbf{Q}\cdot(\mathbf{k}_1 - \mathbf{k}_2) - \mathbf{k}_1\cdot\mathbf{k}_2 .
\end{aligned}$$

Upon integration over $\mathbf{k}_1$ and $\mathbf{k}_2$ the $\mathbf{Q}\cdot(\mathbf{k}_1 - \mathbf{k}_2)$ terms vanish because of the symmetry of the remainder of the integrands. Hence, all left-hand sides in Eq. (6.14) are equal effectively. Identifying the terms of order $\mathcal{O}(1/\overline{M})$, we find the following nonadiabatic corrections.

(i) $N\Delta$ graphs.

$$V_{N\Delta}^{(2)}(\alpha) = - \quad C_{N\Delta}^{(\alpha)}(I)\left(\frac{f_{N\Delta\pi}}{m_\pi}\right)^2\left(\frac{f_{NN\pi}}{m_\pi}\right)^2$$

$$\times \int\int \frac{d^3k_1 d^3k_2}{(2\pi)^6}\, e^{i(\mathbf{k}_1+\mathbf{k}_2)\cdot\mathbf{r}}F(\mathbf{k}_1^2)F(\mathbf{k}_2^2)$$

$$\times \left(\frac{\mathbf{k}_1\cdot\mathbf{k}_2}{2\overline{M}}\right)O_{N\Delta}^{(\alpha)}(\mathbf{k}_1,\mathbf{k}_2)D_\alpha^{(1)\prime\prime}(\omega_1,\omega_2) , \quad (6.15)$$

where $O_{N\Delta}^{(\alpha)}$ can be found in Table I. The energy denominators $D^{(1)\prime\prime}$ are given in the first part of Table V. There we have introduced the splittings $D_X'' = D_{X,a}'' + D_{X,b}'' + D_{X,c}''$ for the crossed BW graphs in order to distinguish the various contributions. The TMO contributions are not given, since they are $\mathcal{O}(1/M^2)$.

In order to evaluate the potentials, it is more convenient to rewrite the expressions for the energy denominators $D^{(1)\prime\prime}$ in a form such that the results of Appendices B and C can be applied to do the integrations in Eq. (6.15). We find

$$D_{//}'' = \frac{1}{2\omega_1\omega_2}\left[\frac{1}{(\omega_1+a)^2\omega_2^2} + \frac{1}{\omega_1^2(\omega_2+a)^2} + \frac{a}{\omega_1(\omega_1+a)^2}\frac{1}{\omega_2(\omega_2+a)} + \frac{1}{\omega_1(\omega_1+a)}\frac{a}{\omega_2(\omega_2+a)^2}\right.$$

$$\left. -a\frac{d}{da}a\left(\frac{1}{\omega_1(\omega_1+a)\omega_2^2(\omega_2+a)} + \frac{1}{\omega_1^2(\omega_1+a)\omega_2(\omega_2+a)} - \frac{1}{\omega_1\omega_2(\omega_1+a)(\omega_2+a)}\frac{2}{\omega_1+\omega_2}\right)\right] \quad (6.16)$$

$$D_{X,a}'' = \frac{1}{2\omega_1^3\omega_2^3}\frac{\omega_1^2 + \omega_2^2 - \omega_1\omega_2 + a(\omega_1+\omega_2)}{(\omega_1+a)(\omega_2+a)} - \frac{a}{\omega_1^2\omega_2^2(\omega_1+a)(\omega_2+a)(\omega_1+\omega_2)}$$

$$-\frac{d}{da}\left\{\frac{\omega_1+\omega_2+a}{2\omega_1^2\omega_2^2(\omega_1+a)(\omega_2+a)}\right\} + \frac{d}{da}\left\{\frac{1}{\omega_1\omega_2(\omega_1+a)(\omega_2+a)(\omega_1+\omega_2)}\right\} \quad (6.17)$$

$$D_{X,b}'' + D_{X,c}'' = \frac{1}{\omega_1^2(\omega_1+a)}\frac{1}{\omega_2^2(\omega_2+a)} + \frac{1}{2\omega_1(\omega_1+a)\omega_2^2(\omega_2+a)^2} + \frac{1}{2\omega_1^2\omega_2^3(\omega_2+a)}$$

$$+ \frac{1}{2\omega_1^2(\omega_1+a)^2\omega_2(\omega_2+a)} + \frac{1}{2\omega_1^3(\omega_1+a)\omega_2^2} . \quad (6.18)$$

Note that all denominators with $\omega_1+\omega_2+a$ have cancelled against similar factors in the numerators. Using these expressions, the integrals are easy to do. We find

$$V_{N\Delta}^{(2)}(\mathrm{BW}_{//}) = + \; C_{N\Delta}^{(//)}(I)\left(\frac{f_{N\Delta\pi}}{m_\pi}\right)^2\left(\frac{f_{NN\pi}}{m_\pi}\right)^2\frac{1}{2\overline{M}}$$

$$\times \lim_{r_1\to r_2}(\boldsymbol{\nabla}_1\cdot\boldsymbol{\nabla}_2)O_{N\Delta}^{(//)}(-i\boldsymbol{\nabla}_1,-i\boldsymbol{\nabla}_2)$$

$$\times B_1(r_1,r_2) , \quad (6.19)$$

where

$$B_1(r_1,r_2) = G_{1,2}(r_1)I_3(r_2) + aG_{2,2}(r_1)G_{2,1}(r_2)$$

$$+a\frac{d}{da}a\left[H_{2,2}(r_1,r_2) - G_{2,1}(r_1)G_{3,1}(r_2)\right] , \quad (6.20)$$

where we have made use of the symmetry $r_1 \leftrightarrow r_2$

to write Eq. (6.20) in a concise form. Here, we have also suppressed the a dependence of $G_{n,m}$ and $H_{n,m}$ for notational reasons. The differentiations and limits can be worked out using Eqs. (C11) and (C12) in a straightforward manner, which comes down to inserting the $\odot$ operation defined in Appendix C between the r_1- and r_2-dependent functions in $B_1(r_1,r_2)$. This is completely analogous to the evaluation of Eq. (6.5) to, e.g., Eq. (6.10) as discussed in Sec. VI A.

In a similar way, for the crossed BW graphs we find

$$V_{N\Delta}^{(2)}(\mathrm{BW}_X) = + \; C_{N\Delta}^{(X)}(I)\left(\frac{f_{N\Delta\pi}}{m_\pi}\right)^2\left(\frac{f_{NN\pi}}{m_\pi}\right)^2\frac{1}{2\overline{M}}$$

$$\times \lim_{r_1\to r_2}(\boldsymbol{\nabla}_1\cdot\boldsymbol{\nabla}_2)O_{N\Delta}^{(X)}(-i\boldsymbol{\nabla}_1,-i\boldsymbol{\nabla}_2)$$

$$\times B_2(r_1,r_2) , \quad (6.21)$$

with

$$B_2(r_1, r_2) = a\left[G_{2,1}(r_1)G_{3,1}(r_2) - H_{2,2}(r_1, r_2)\right] - \frac{d}{da}\left[G_{1,1}(r_1)G_{2,1}(r_2) + \frac{a}{2}G_{2,1}(r_1)G_{2,1}(r_2) - H_{1,1}(r_1, r_2)\right]$$

$$+ G_{1,1}(r_1)G_{3,1}(r_2) + \tfrac{1}{2}G_{2,1}(r_1)G_{2,1}(r_2) + G_{1,1}(r_1)G_{2,2}(r_2) + G_{3,1}(r_1)I_2(r_2) . \tag{6.22}$$

(ii) $\Delta\Delta$ graphs.

$$V^{(2)}_{\Delta\Delta}(\alpha) = -\, C^{(\alpha)}_{\Delta\Delta}(I)\left(\frac{f_{N\Delta\pi}}{m_\pi}\right)^4$$

$$\times \int\int \frac{d^3k_1\, d^3k_2}{(2\pi)^6}\, e^{i(\mathbf{k}_1+\mathbf{k}_2)\cdot\mathbf{r}}F(\mathbf{k}_1^2)F(\mathbf{k}_2^2)$$

$$\times \left(\frac{\mathbf{k}_1\cdot\mathbf{k}_2}{2M_\Delta}\right)O^{(\alpha)}_{\Delta\Delta}(\mathbf{k}_1, \mathbf{k}_2)D^{(2)'''}_\alpha(\omega_1, \omega_2) \tag{6.23}$$

where $O^{(\alpha)}_{\Delta\Delta}$ can be found in Table I. The energy denominators $D^{(2)'''}$ are given in the second part of Table V, where we have already used a little algebra to bring the contributions from the crossed graphs in a convenient form. Note that again all denominators with $\omega_1 + \omega_2 + 2a$ are cancelled against similar factors in the numerators. Evaluating the integrals, we find for the planar BW graph

$$V^{(2)}_{\Delta\Delta}(\mathrm{BW}_{//}) = +\, C^{(//)}_{\Delta\Delta}(I)\left(\frac{f_{N\Delta\pi}}{m_\pi}\right)^4 \frac{1}{2M_\Delta}$$

$$\times \lim_{\mathbf{r}_1\to\mathbf{r}_2}(\nabla_1\cdot\nabla_2)O^{(//)}_{\Delta\Delta}(-i\nabla_1, -i\nabla_2)$$

$$\times C_1(r_1, r_2) , \tag{6.24}$$

where

$$C_1(r_1, r_2) = -\frac{1}{2}\frac{d}{da}H_{1,1}(r_1, r_2) . \tag{6.25}$$

Similarly, for the crossed BW graphs

$$V^{(2)}_{\Delta\Delta}(\mathrm{BW}_X) = +\, C^{(X)}_{\Delta\Delta}(I)\left(\frac{f_{N\Delta\pi}}{m_\pi}\right)^4 \frac{1}{2M_\Delta}$$

$$\times \lim_{\mathbf{r}_1\to\mathbf{r}_2}(\nabla_1\cdot\nabla_2)O^{(X)}_{\Delta\Delta}(-i\nabla_1, -i\nabla_2)$$

$$\times C_2(r_1, r_2) , \tag{6.26}$$

where

$$C_2(r_1, r_2) = \frac{1}{2}\frac{d^2}{da^2}\left[G_{1,1}(r_1)G_{1,1}(r_2) + aH_{1,1}(r_1, r_2)\right] . \tag{6.27}$$

All differentiations and limits can be easily worked out again using Eqs. (C11) and (C12).

VII. RESULTS AND DISCUSSION

The complete TPEP for the $N\Delta$ and $\Delta\Delta$ graphs for a single-channel calculation for the NN system can be

TABLE V.   Nonadiabatic approximation of the energy denominators $D^{(1)''}_\alpha$ for $N\Delta$ and $D^{(2)''}_\alpha$ for $\Delta\Delta$ intermediate states.

α	$D^{(1)''}_\alpha(\omega_1, \omega_2)$
BW$_{//}$	$\dfrac{1}{2\omega_1\omega_2}\left[\dfrac{1}{(\omega_1+a)^2}\dfrac{1}{\omega_2} + \dfrac{1}{\omega_1}\dfrac{1}{(\omega_2+a)^2} + \dfrac{1}{(\omega_1+a)}\dfrac{1}{\omega_2^2} + \dfrac{1}{\omega_1^2}\dfrac{1}{(\omega_2+a)}\right]\dfrac{1}{(\omega_1+\omega_2)}$
BW$_{X,a}$	$\dfrac{1}{2\omega_1\omega_2}\left[\dfrac{1}{(\omega_1+a)^2}\dfrac{1}{\omega_1} + \dfrac{1}{\omega_2}\dfrac{1}{(\omega_2+a)^2} + \dfrac{1}{(\omega_1+a)}\dfrac{1}{\omega_1^2} + \dfrac{1}{\omega_2^2}\dfrac{1}{(\omega_2+a)}\right]\dfrac{1}{(\omega_1+\omega_2)}$
BW$_{X,b}$	$\dfrac{1}{2\omega_1\omega_2}\left[\left\{\dfrac{1}{(\omega_1+a)^2}\dfrac{1}{\omega_1} + \dfrac{1}{\omega_2}\dfrac{1}{(\omega_2+a)^2} + \dfrac{1}{(\omega_1+a)}\dfrac{1}{\omega_1^2} + \dfrac{1}{\omega_2^2}\dfrac{1}{(\omega_2+a)}\right\}\dfrac{1}{(\omega_1+\omega_2+a)}\right.$ $\left. + \left\{\dfrac{1}{(\omega_1+a)}\dfrac{1}{\omega_1} + \dfrac{1}{\omega_2}\dfrac{1}{(\omega_2+a)}\right\}\dfrac{2}{(\omega_1+\omega_2+a)^2}\right]$
BW$_{X,c}$	$\dfrac{1}{2\omega_1\omega_2}\left[\left\{\dfrac{1}{\omega_1^2\omega_2} + \dfrac{1}{\omega_1\omega_2^2} + \dfrac{1}{(\omega_1+a)^2(\omega_2+a)} + \dfrac{1}{(\omega_1+a)(\omega_2+a)^2}\right\}\dfrac{1}{(\omega_1+\omega_2+a)}\right.$ $\left. + \left\{\dfrac{1}{\omega_1\omega_2} + \dfrac{1}{(\omega_1+a)(\omega_2+a)}\right\}\dfrac{2}{(\omega_1+\omega_2+a)^2}\right]$

α	$D^{(2)''}_\alpha(\omega_1, \omega_2)$
BW$_{//}$	$-\dfrac{1}{2\omega_1\omega_2}\dfrac{d}{da}\left[\dfrac{1}{(\omega_1+a)(\omega_2+a)}\dfrac{1}{\omega_1+\omega_2}\right]$
BW$_X$	$\dfrac{1}{2\omega_1\omega_2}\dfrac{d^2}{da^2}\left[\dfrac{1}{(\omega_1+a)(\omega_2+a)} + \dfrac{a}{(\omega_1+a)(\omega_2+a)}\dfrac{1}{\omega_1+\omega_2}\right]$

written as

$$V(\text{TPE}) = \sum_{i=0}^{2} V^{(i)}(\text{BW}) + V^{(i)}(\text{TMO}) + V^{(i)}(\text{Born}),$$

(7.1)

where BW contains the planar- and crossed-box contributions, and each potential consists of a central, spin-spin, tensor, and spin-orbit part. The relevant expressions can be found in Sec. V for $V^{(0)}$, in Sec. VI A for $V^{(1)}$, and in Sec. VI B for $V^{(2)}$. The inclusion of the Born term $V^{(i)}(\text{Born})$ is due to our special definition of the TMO potential, Eq. (4.12), which explicitly includes the subtraction of the once-iterated OPE. For a coupled-channel calculation this Born term should be left out.

In Figs. 10–15 the results for the several potentials and several of the different contributions are shown. In these numerical results we have evaluated the TPEP for $f_{NN\pi}^2/4\pi = 0.075$ from the Nijmegen partial-wave analysis [32], $f_{N\Delta\pi}^2/4\pi = 0.35$ from the Δ_{33} isobar decay width, and $\Lambda = 664.52$ MeV. Of course, due to the Gaus-

sian form factors all potentials are finite at $r = 0$ and rather soft. When not stated explicitly otherwise, we have evaluated the potentials for $T_{\text{lab}} = 150$ MeV. We have also tacitly assumed that the strong form factor for the nucleon and the Δ_{33} isobar are the same, which need not be the case, of course.

In Figs. 10 (a)–(d) we show the total Δ-isobar contributions, due to the $N\Delta$ and $\Delta\Delta$ intermediate states, the contributions from the NN intermediate states, and the total TPEP. This for the central, spin-spin, and tensor potentials. Noteworthy is the strong cancellation between the isobar and the nonisobar potentials for $I = 0$. Tuning, for example, the $N\Delta\pi$ coupling constant could make these cancellations almost complete. For $I = 1$, on the other hand, the isobar and nonisobar contributions reinforce each other. The total potentials resemble a mixture of about 70% isoscalar and 30% isovector exchange.

In Figs. 11 (a)–(d) the $N\Delta$ and $\Delta\Delta$ intermediate-state contributions to the central, spin-spin, and tensor potentials are shown. In the central potential, the $\Delta\Delta$ contribution is important, in particular, for the $I = 0$ case. The
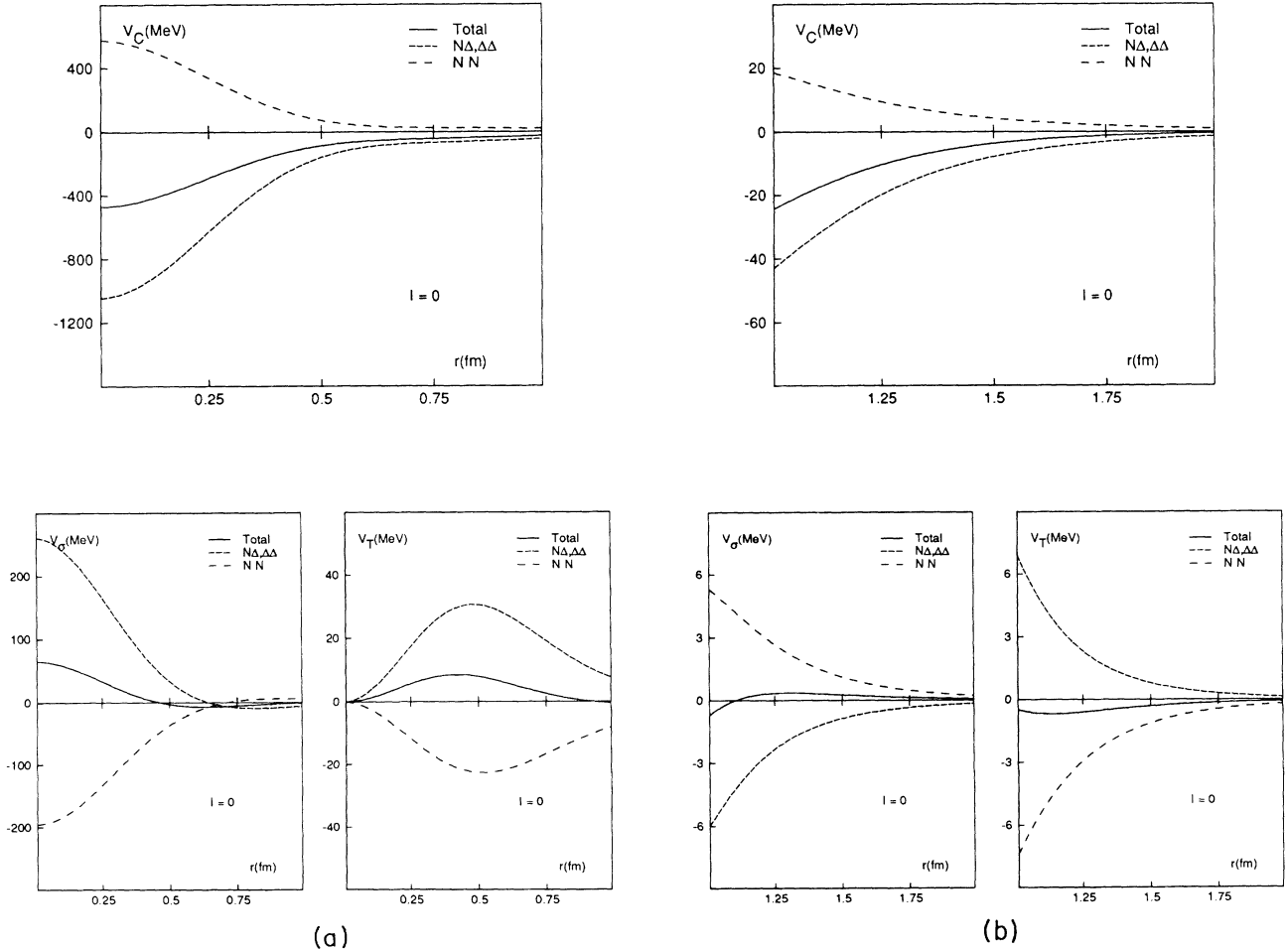
FIG. 10. TPEP central, spin-spin, and tensor contributions due to NN, or $N\Delta$ and $\Delta\Delta$ intermediate states. The total contribution is also shown. (a) $I = 0$ and $r \leq 1$ fm; (b) $I = 0$ and $1 \leq r \leq 2$ fm; (c) $I = 1$ and $r \leq 1$ fm; (d) $I = 1$ and $1 \leq r \leq 2$ fm.

total central potential has an isoscalar exchange character. The spin-spin and tensor potentials are dominated by the $N\Delta$ contribution and are dominantly isovector exchange.

In Figs. 12 (a)–(b) the BW, the TMO, and the Born contributions are compared. The $I = 0$ channel is strongly dominated by the BW graphs. This is natural since only the $\Delta\Delta$ intermediate state can contribute for TMO and Born. In the $I = 1$ channel this is no longer the case. As far as the short-range part is concerned, there appear large cancellations between the TMO and the Born contributions below $r = 1$ fm.

In Figs. 13 (a)–(b) the $V^{(0)}$, $V^{(1)}$, and $V^{(2)}$ potentials are compared. For $r \geq 1$ fm, $V^{(0)}$ clearly dominates. This is also the case at very short range. In $I = 1$ there are large cancellations between the $N\Delta$ and the $\Delta\Delta$ contributions for the spin-spin and the tensor potentials, which result in extremely small contributions.

In Figs. 14 (a)–(b) the spin-orbit potentials are shown. The tail of the spin-orbit potential from the $1/M$ term in the pseudovector vertex is positive and much larger than for the TPEP from the NN intermediate states [1]. It is also stronger than that from the heavy-boson exchange

(HBE) (see [1]). Moreover, this spin orbit is not like that from scalar exchange. As can be seen from the figures, the central potentials are dominantly $I = 0$ exchange, whereas the spin-spin and the tensor potentials are dominantly $I = 1$ exchange. Therefore, the central potential could be described by the exchange of an effective scalar meson. The corresponding spin-orbit potential, which is purely the Thomas term [31], can be obtained from the formula

$$V_{SO}(r) \approx -\frac{1}{2M_N^2}\frac{1}{r}\frac{d}{dr}V_C^{(0)}(r) \; , \tag{7.2}$$

where we have included only the dominant contribution to V_C. In Fig. 14 both the Thomas and the pseudovector-correction contributions are shown together with their sum. Beyond $r = 1$ fm there is virtually a complete cancellation of the spin-orbit contributions.

In Figs. 15 (a) and (b) the energy dependence of the once-iterated Born term contributions are shown. We give the curves for $T_{\text{lab}} = 0, 150, 350$ MeV, respectively. As can be seen from these curves, the energy dependence is very mild. The TMO potentials show a similar behavior.
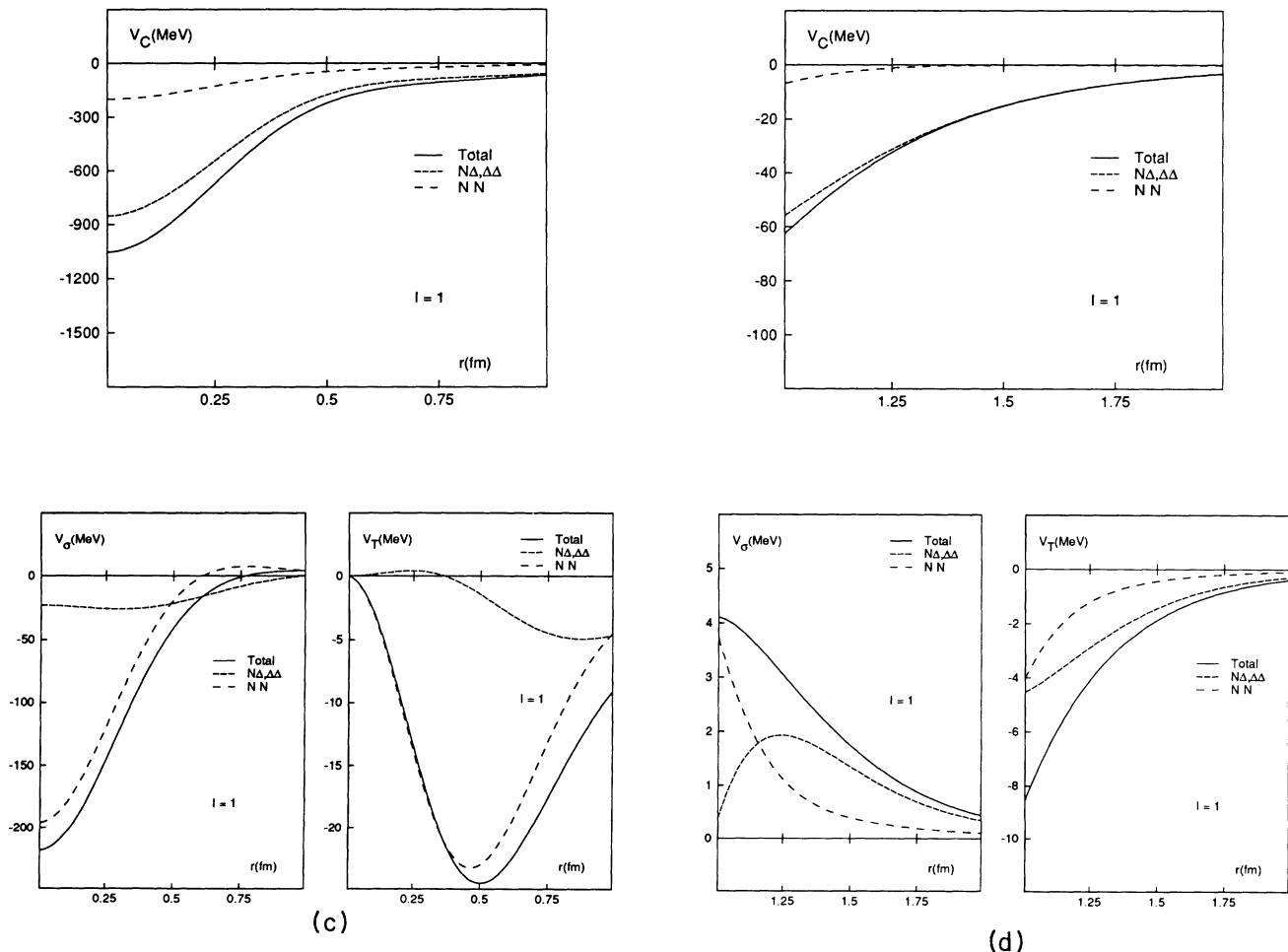
FIG. 10. (Continued).

The actual choice we made for Λ in Figs. 10 to 15 is not totally arbitrary. First of all, it has the same value as used in the figures of [1]. Furthermore, a low value for the $NN\pi$ form factor ($\Lambda \approx 770$ MeV) seems to be preferred with regard to the Goldberger-Treiman relation and some recent NN and $\overline{N}N$ partial-wave analyses [32, 33]. Here we only consider it as an effective parameter, which in a later stage should be determined by a confrontation with the data. In Fig. 16 we show the effect of the form factor. The value $\Lambda = 964.52$ MeV is the value found in Ref. [2] in a fit to the NN data. One sees that the tail of the $I = 1$ potential starts at $r \approx 1.5$ fm. The same is true for the $I = 0$ potential.

As compared to the isobar TPEP's in the literature, the tail of our potentials are roughly the same as those of Chemtob et al. [9]. Of course, the intermediate and inner regions are very different because they do not include any form factors. The differences between [9] and this paper can be seen clearly by comparing the results for the NN-box diagrams. In [9] the $NN\pi$ pseudoscalar (ps) coupling was used in contrast to the pseudovector (pv) coupling in the present paper. Moreover, we ne-

glect the pv-pair terms which are an order of magnitude smaller than those from the ps coupling. So the differences between [9] and our work are mainly due to the pair terms. Indeed, the latter explain the different tails completely. This is demonstrated in Fig. 17 for the TPEP with NN intermediate states. The curve labeled "no-pair" (corresponding to the ps-pv theory) represents our $\gamma_\mu\gamma_5$ theory, assuming strong pair suppression. Adding the dashed curve labeled "pairs," which represents the pair terms of the γ_5 theory [34], results in the solid curve of the ps-ps theory. A similar behavior is shown when we include the pair terms of the TPEP with $N\Delta$ and $\Delta\Delta$ intermediate states.

ACKNOWLEDGMENTS
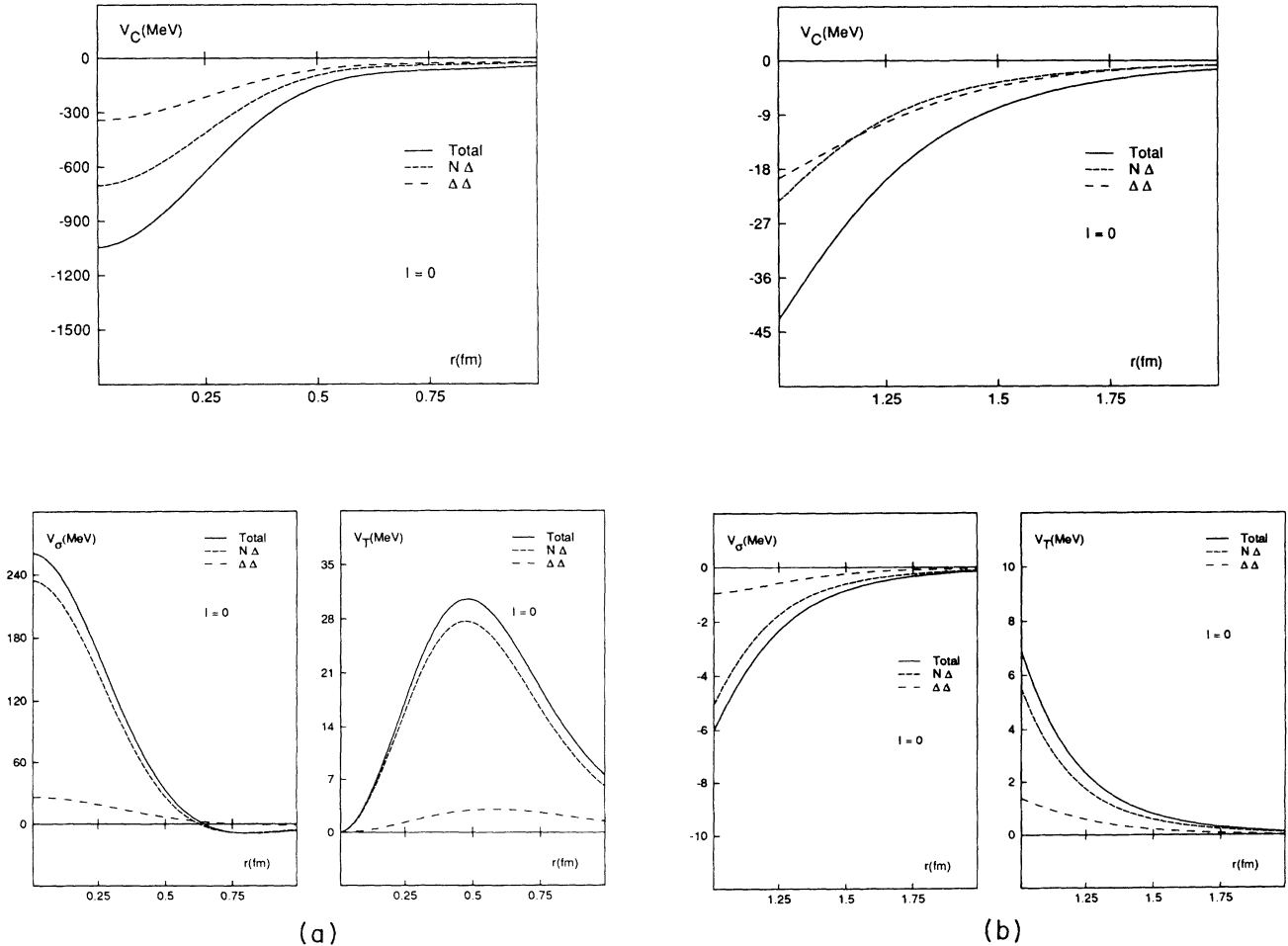
FIG. 11. Separate TPEP central, spin-spin, and tensor contributions due to $N\Delta$ and $\Delta\Delta$ intermediate states for $I = 0$ and $I = 1$. Contributions (a)–(d) as in Fig. 10.

the Nederlandse Organisatie voor Wetenschappelijk Onderzoek (NWO).

APPENDIX A: TREATMENT TMO AND BORN ITERATION

The *NN*- and *N*Δ-threshold difference causes special problems in the treatment of the TMO graphs and the Born iteration. Making the nonadiabatic expansion of the energy denominator for the *N*Δ intermediate state in the kernels (4.4a) and (4.4b), one gets

$$(\mathcal{E}_{\mathbf{p}-\mathbf{k}_1} + E_{\mathbf{p}-\mathbf{k}_1} - W)^{-1} \approx (a - \beta_1)^{-1} , \qquad \text{(A1)}$$

with $a = M_\Delta - M_N$ and $\beta_1 = \mathbf{k}_1 \cdot \mathbf{k}_2/\overline{M}$, where $\overline{M} = (M_\Delta + M_N)/2$. In order not to limit the applicability of our formulas to the very low energy region, we avoid the expansion of the denominator (A1) as a power series in β_1. Restricting ourselves to energies below the *N*Δ threshold (so $a - \beta_1 > 0$), we write

$$\frac{1}{a - \beta_1} = \int_0^\infty dz e^{-z(a-\beta_1)} . \qquad \text{(A2)}$$

Using

$$\beta_1 = \frac{\mathbf{k}_1 \cdot \mathbf{k}_2}{\overline{M}} = \frac{1}{2\overline{M}} \left(\mathbf{k}^2 - \mathbf{k}_1^2 - \mathbf{k}_2^2\right) , \qquad \text{(A3)}$$

we get in combination with the Gaussian form factors

$$\frac{F_1(\mathbf{k}_1^2)F_2(\mathbf{k}_2^2)}{(a - \beta_1)}$$

$$= \int_0^\infty dz \exp[-z(a - \mathbf{k}^2/2\overline{M})]$$
$$\times \exp\left[-\mathbf{k}_1^2/\Lambda_1^2(z)\right] \exp\left[-\mathbf{k}_2^2/\Lambda_2^2(z)\right] . \qquad \text{(A4)}$$

Here

$$\Lambda(z) = \Lambda \left(1 + \frac{\Lambda^2}{2\overline{M}}z\right)^{-1/2} . \qquad \text{(A5)}$$
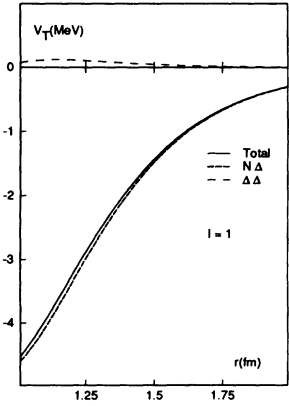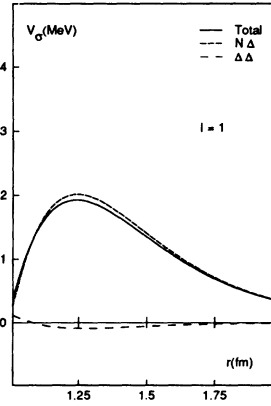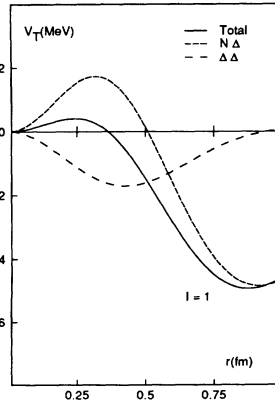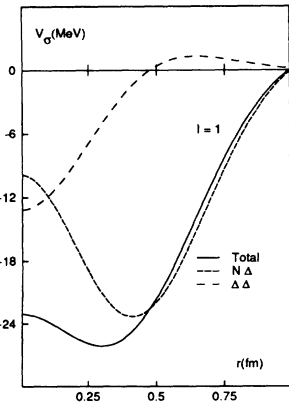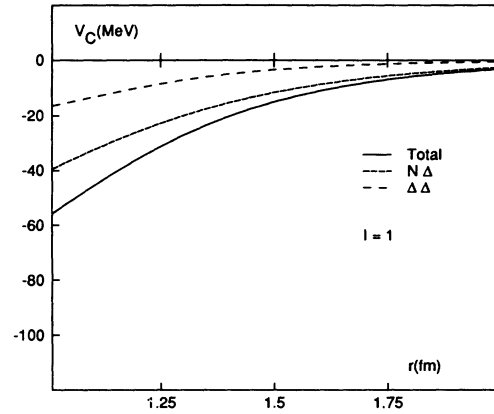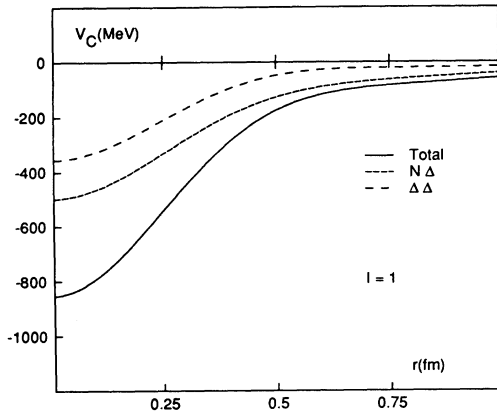
(c)

(d)

FIG. 11. (*Continued*).

In making the nonadiabatic expansion in the other energy denominators in the kernels (4.4a) and (4.4b) for the TMO graphs, and after subtracting the OPE iteration, we obtain terms of the form $\beta_1/(a - \beta_1)$, which we write as

$$\frac{\beta_1}{a - \beta_1} = -1 + \frac{a}{a - \beta_1} \ .$$

The term on the right-hand side in the limit $a \to 0$ corresponds to the TMO potentials with NN intermediate states [1]. This contribution will therefore be included in $V_{\text{TMO}}^{(0)}$.

To the second term on the right-hand side we apply the procedure described in the following. The contribution to the nucleon-nucleon potential will essentially be of the general form [cf. Eq. (A4)]

$$V(r) = \int \int \frac{d^3 k_1 d^3 k_2}{(2\pi)^6} \ e^{i(\mathbf{k}_1 + \mathbf{k}_2) \cdot \mathbf{r}}$$

$$\times a \int_0^\infty dz e^{-z(a - \mathbf{k}^2/2\overline{M})} F(z; \mathbf{k}_1^2) G(z; \mathbf{k}_2^2)$$

$$= a \int_0^\infty dz e^{-z(a + \Delta/2\overline{M})} V(z; r) \ , \qquad \text{(A6)}$$

where the Laplacian Δ operates on $V(z; r)$ only. Operating with $V(r)$ on the NN wave function $\psi(r)$ gives

$$V(r)\psi(r) = a \int_0^\infty dz e^{-z(a + \Delta/2\overline{M})} V(z; r)\psi(r)$$

$$\approx a \int_0^\infty dz e^{-z(a - \frac{1}{2} T_{\text{lab}})} \widetilde{V}(z; r)\psi(r) \ , \quad \text{(A7)}$$

where
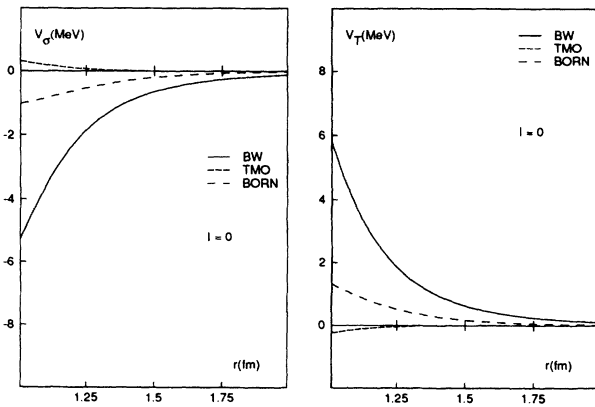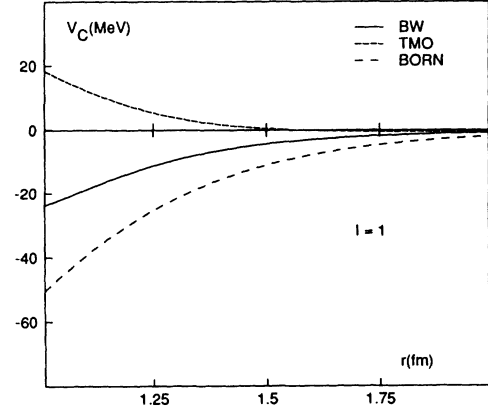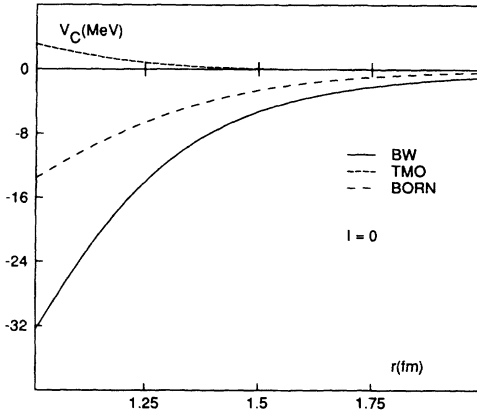
(a)
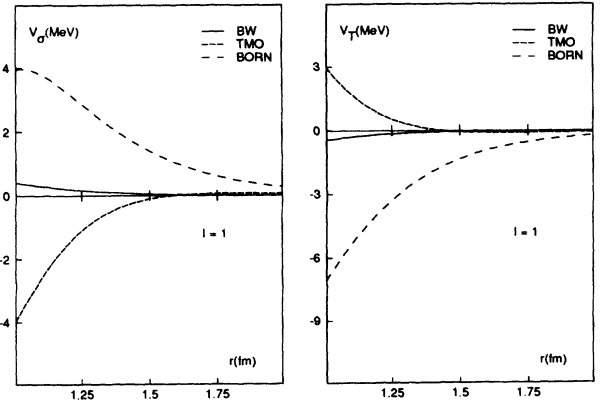
(b)

FIG. 12.   Isobar TPE central, spin-spin, and tensor contributions to the potential tail of the BW, TMO, and Born diagrams for (a) $I = 0$ and (b) $I = 1$.

$$\tilde{V}(z;r) = e^{-z\Delta/2\overline{M}} V(z;r) e^{z\Delta/2\overline{M}}$$

$$= V(z;r) + z \left[V(z;r), \frac{\Delta}{2\overline{M}} \right] + \cdots$$

$$\approx V(z;r) . \qquad (A8)$$

Moreover, in Eq.(A7) we used the Schrödinger equation $(-\Delta/\overline{M} + V_{NN})\psi \approx T_{\mathrm{lab}}\psi$ and neglected the NN potential V_{NN}. We believe this is a reasonable approximation since the total potential is in general rather weak. The alternative would be to use some average potential. In Eq. (A7), the integrand clearly shows that our formulas are limited to the region below the $N\Delta$ threshold. This occurs at $T_{\mathrm{lab}} = 2a \approx 600$ MeV.

The treatment of the $\Delta\Delta$ intermediate state is similar to that for the $N\Delta$ intermediate states described above, except that a is to be replaced by $2a$ and β_1 by $\beta_2 = \mathbf{k}_1 \cdot \mathbf{k}_2 / M_\Delta$.

APPENDIX B: INTEGRAL REPRESENTATIONS

We give a catalog of integral representations for the energy denominators which occur in the potentials in momentum space. The techniques used are similar to those given in Appendix B of Ref. [1]. We start from the basic representations $(a > 0)$

$$\frac{1}{\omega} = \frac{2}{\pi} \int_0^\infty \frac{d\lambda}{\omega^2 + \lambda^2} , \qquad (B1a)$$

$$\frac{1}{\omega + a} = \frac{2}{\pi} \int_0^\infty \frac{\lambda^2 \, d\lambda}{(\omega^2 + \lambda^2)(a^2 + \lambda^2)} , \qquad (B1b)$$

where $\omega = \omega(\mathbf{k}) = \sqrt{\mathbf{k}^2 + \mu^2}$, and derive from these the following formulas by simple fraction splitting and/or differentiation:

(a)

(b)
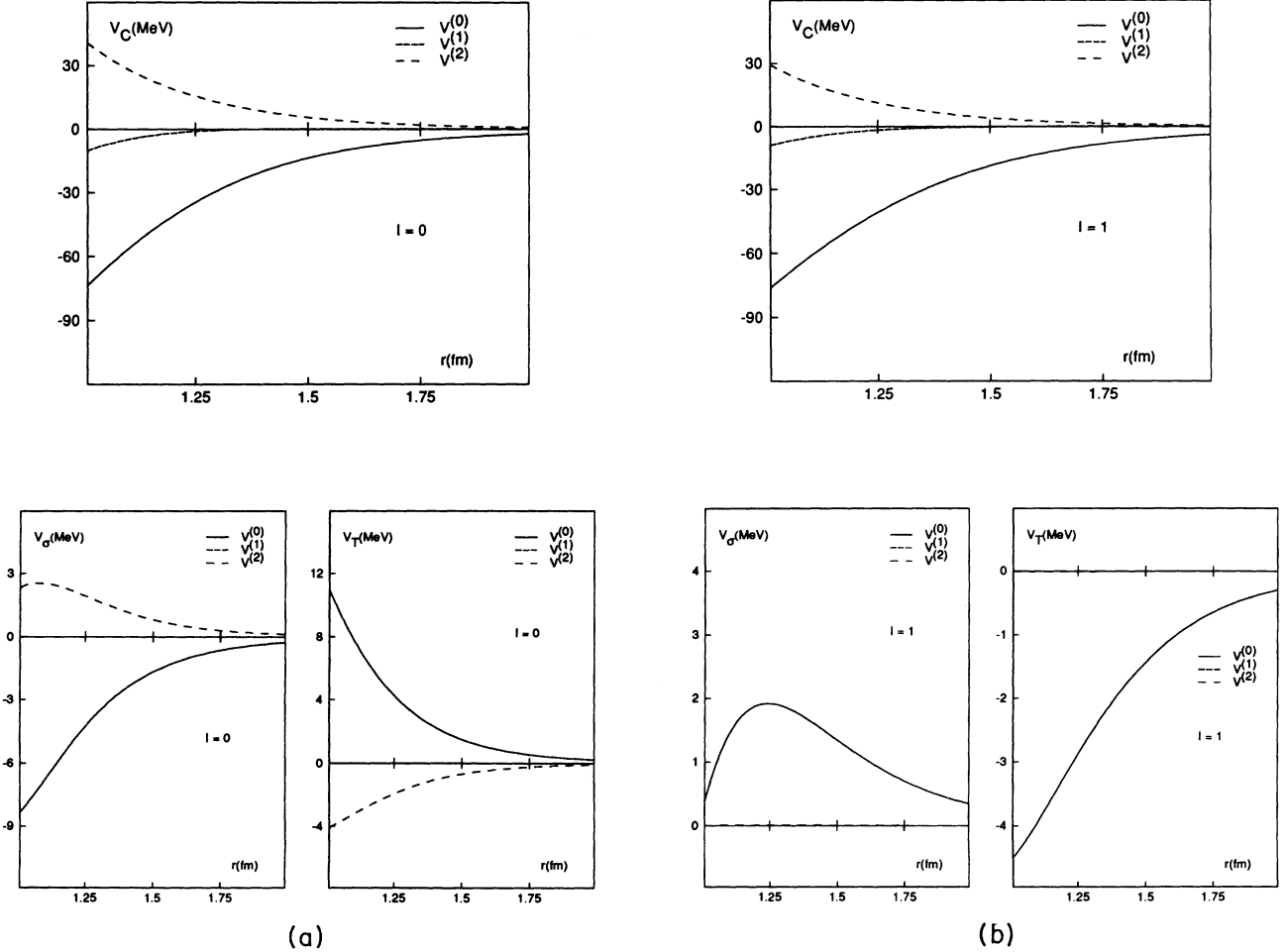
FIG. 13. The $V^{(0)}$, $V^{(1)}$, and $V^{(2)}$ contributions of the isobar TPE central, spin-spin, and tensor potential tails for (a) $I = 0$ and (b) $I = 1$.

$$\frac{1}{\omega}\frac{1}{\omega + a} = \frac{2a}{\pi} \int_0^\infty \frac{d\lambda}{(\omega^2 + \lambda^2)(a^2 + \lambda^2)} \ ,$$

$$\frac{1}{(\omega + a)^2} = \frac{4a}{\pi} \int_0^\infty \frac{\lambda^2 d\lambda}{(\omega^2 + \lambda^2)(a^2 + \lambda^2)^2} \ ,$$

$$\text{(B2)}$$

$$\frac{1}{\omega^2}\frac{1}{(\omega + a)} = \frac{1}{a}\left(\frac{1}{\omega^2} - \frac{2a}{\pi}\int_0^\infty \frac{d\lambda}{(\omega^2 + \lambda^2)(a^2 + \lambda^2)}\right),$$

$$\frac{1}{\omega}\frac{1}{(\omega + a)^2} = \frac{2}{\pi}\int_0^\infty d\lambda \frac{(a^2 - \lambda^2)}{(\omega^2 + \lambda^2)(a^2 + \lambda^2)^2} \ .$$

The basic Fourier transformation for OPE with a Gaussian form factor is

$$I_2(m, r) \equiv (2\pi)^{-3} \int d^3k \ e^{i\mathbf{k}\cdot\mathbf{r}} \ \tilde{I}_2(\mathbf{k}^2) \ ,$$

$$\text{(B3)}$$

$$\tilde{I}_2(\mathbf{k}^2) = \int_0^\infty d\mu^2 \frac{\rho(\mu^2)}{\mathbf{k}^2 + \mu^2} \simeq \frac{e^{-\mathbf{k}^2/\Lambda^2}}{\mathbf{k}^2 + m^2} \ ,$$

where in the last equation we used the substitution (4.8). In terms of the error functions [35], this transformation has been given explicitly in Ref. [2] and it reads

$$I_2(m, r) = \frac{m}{4\pi}\phi_C^0(m, r)$$

$$\text{(B4)}$$

$$\phi_C^0(m, r) = e^{m^2/\Lambda^2}\left[e^{-mr}\text{erfc}\left(-\frac{\Lambda r}{2} + \frac{m}{\Lambda}\right)\right.$$
$$\left. - e^{mr}\text{erfc}\left(\frac{\Lambda r}{2} + \frac{m}{\Lambda}\right)\right]\frac{1}{2mr} \ .$$

The derivatives are easy to obtain and we list

$$\frac{d}{dr}\phi_C^0(m, r) = -m^2 r\phi_{SO}^0(m, r) \ ,$$

$$\frac{d^2}{dr^2}\phi_C^0(m, r) = m^2\phi_C^1(m, r) + 2m^2\phi_{SO}^0(m, r) \ ,$$

$$\frac{d^3}{dr^3}\phi_C^0(m, r) = -m^4 r\phi_{SO}^1(m, r) - \frac{6m^2}{r}\phi_T^0(m, r) \ ,$$
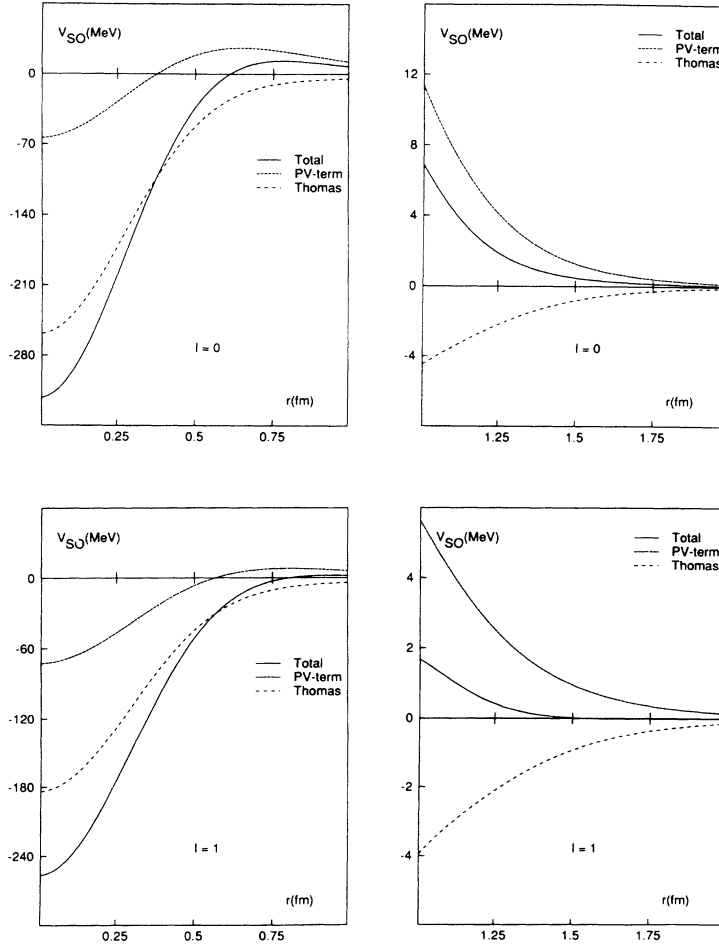
FIG. 14. Spin-orbit potential contributions to the isobar TPE potentials for (a) $r \leq 1$ fm and (b) $1 \leq r \leq 2$ fm.

where ϕ_X^n can be found in Refs. [2, 3]. Above, we have written all the occurring forms of energy denominators in such a way that the Fourier transformation of Eq. (B3) given in Eq. (B4) is sufficient to handle all cases that we will encounter in this paper. For example, the Fourier transformation of Eq. (B1b) is, using Eqs. (B4) and (4.8),

$$I_1(a;r) = \frac{2}{\pi} \int_0^\infty \frac{\lambda^2 d\lambda}{(a^2 + \lambda^2)} I_2(\sqrt{m^2 + \lambda^2}, r) e^{-\lambda^2/\Lambda^2} .$$

(B5)

The Fourier transformation of Eq. (B1a) is obviously $I_1(r) \equiv I_1(0;r)$, while for the higher powers $(\omega + a)^{-n}$ we find $I_n(a;r) = -(d/da)I_{n-1}(a;r)$. In the formulas for the potentials we sometimes use for brevity the notation

$$e^{-\lambda^2/\Lambda^2} I_2(\sqrt{m^2 + \lambda^2}, r) \equiv F(\lambda, r) .$$

(B6)

The double Fourier transformations can be carried through without difficulty once the dependence on $\mathbf{k}_1$ and $\mathbf{k}_2$ is factorized directly or under a λ integral. This can always be achieved by using the identities given above.

(Compare with the procedures as described in Appendix B of Ref. [1].) Also, the application of the above formulas in the presence of (Gaussian) form factors is completely analogous to the TPEP derivation in the case of two nucleons in the intermediate states $(a = 0)$ as given in Ref. [1]. To illustrate the method in more detail, we consider as an example the following typical integral:

$$\tilde{J}_1(\mathbf{k}_1, \mathbf{k}_2) = \int_0^\infty d\mu_1^2 \int_0^\infty d\mu_2^2 \, \frac{\rho(\mu_1^2)\rho(\mu_2^2)}{[\omega(\mathbf{k}_1) + \omega(\mathbf{k}_2)]}$$
$$\times \frac{1}{[\omega(\mathbf{k}_1) + a][\omega(\mathbf{k}_2) + a]},$$

(B7)

which is the analog of the expression (B.10) of Ref. [1]. Here, we can use also the trick of Lévy [36] by writing

$$\frac{1}{(\omega_1 + a)(\omega_2 + a)} \frac{1}{\omega_1 + \omega_2} = \frac{1}{\omega_1^2 - \omega_2^2}$$
$$\times \left(\frac{1}{\omega_2 + a} - \frac{1}{\omega_1 + a} \right) .$$

(B8)
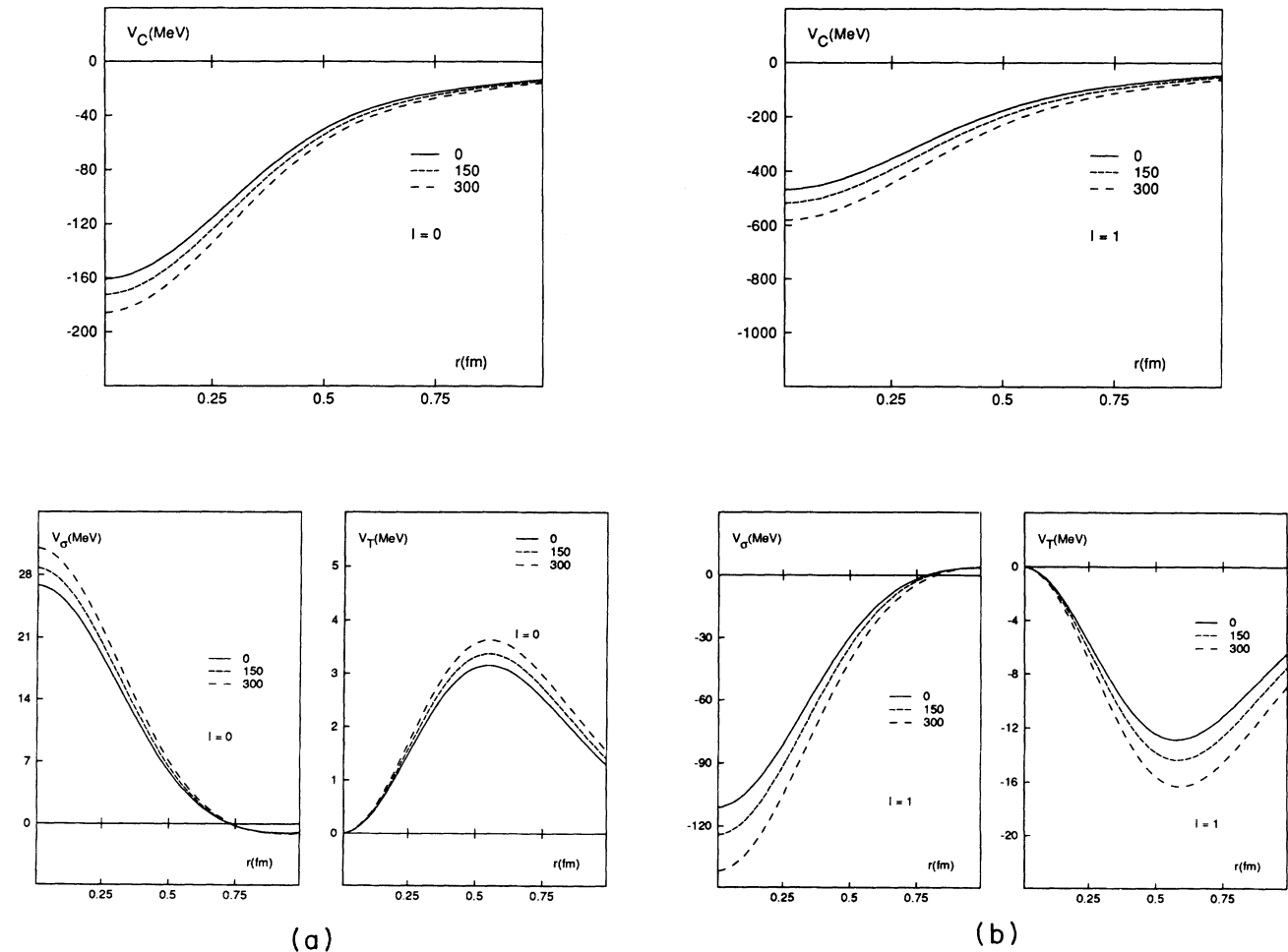
FIG. 15. Energy dependence of the once-iterated Born diagrams to the short- and intermediate-range isobar central, spin-spin, and tensor TPEP's for (a) $I = 0$ and (b) $I = 1$.

Then, with Eq. (B1b) we find the important result

$$\frac{1}{(\omega_1 + a)(\omega_2 + a)}\frac{1}{\omega_1 + \omega_2} = \frac{2}{\pi}\int_0^\infty \frac{\lambda^2 d\lambda}{(a^2 + \lambda^2)}$$

$$\times \frac{1}{(\omega_1^2 + \lambda^2)(\omega_2^2 + \lambda^2)} , \quad (B9)$$

which is the very cornerstone for achieving the separation of the ω_1 and ω_2 dependence and which enables us to do the momentum integrations in an elegant manner. Substituting Eq. (B9) into Eq. (B7) we obtain a factorization of $\mathbf{k}_1$ and $\mathbf{k}_2$ under the λ integral:

$$\tilde{J}_1(\mathbf{k}_1, \mathbf{k}_2) = \frac{2}{\pi}\int_0^\infty \frac{\lambda^2 d\lambda}{(a^2 + \lambda^2)}\left[\int_0^\infty d\mu_1^2 \frac{\rho(\mu_1^2)}{\omega(\mathbf{k}_1)^2 + \lambda^2}\right]$$

$$\times \left[\int_0^\infty d\mu_2^2 \frac{\rho(\mu_2^2)}{\omega(\mathbf{k}_2)^2 + \lambda^2}\right] ,$$

where $\omega(\mathbf{k}_1) = \sqrt{\mathbf{k}_1^2 + \mu_1^2}$ and $\omega(\mathbf{k}_2) = \sqrt{\mathbf{k}_2^2 + \mu_2^2}$. Using the substitution (4.8), we get

$$\tilde{J}_1(\mathbf{k}_1, \mathbf{k}_2) = \frac{2}{\pi}\int_0^\infty \frac{\lambda^2 d\lambda}{(a^2 + \lambda^2)}\left[\frac{e^{-(\mathbf{k}_1^2 + \lambda^2)/\Lambda^2}}{\mathbf{k}_1^2 + m^2 + \lambda^2}\right]$$

$$\times \left[\frac{e^{-(\mathbf{k}_2^2 + \lambda^2)/\Lambda^2}}{\mathbf{k}_2^2 + m^2 + \lambda^2}\right] .$$

For the latter expression, the Fourier transformation can readily be performed and yields

$$J_1(a; r) = \frac{2}{\pi}\int_0^\infty \frac{\lambda^2 d\lambda}{(a^2 + \lambda^2)}e^{-2\lambda^2/\Lambda^2}\left[I_2(\sqrt{m^2 + \lambda^2}, r)\right]^2 .$$

$$(B10)$$

All Fourier integrals appearing in the course of the calculation of the TPE potentials can be treated similarly. Note that the tricks, employed here, also work in the case of the two-meson-exchange potentials, where in general the mesons have different masses.

Next we indicate briefly how to use the results of this Appendix to perform the momentum integrations. To evaluate the Fourier transformations of the different
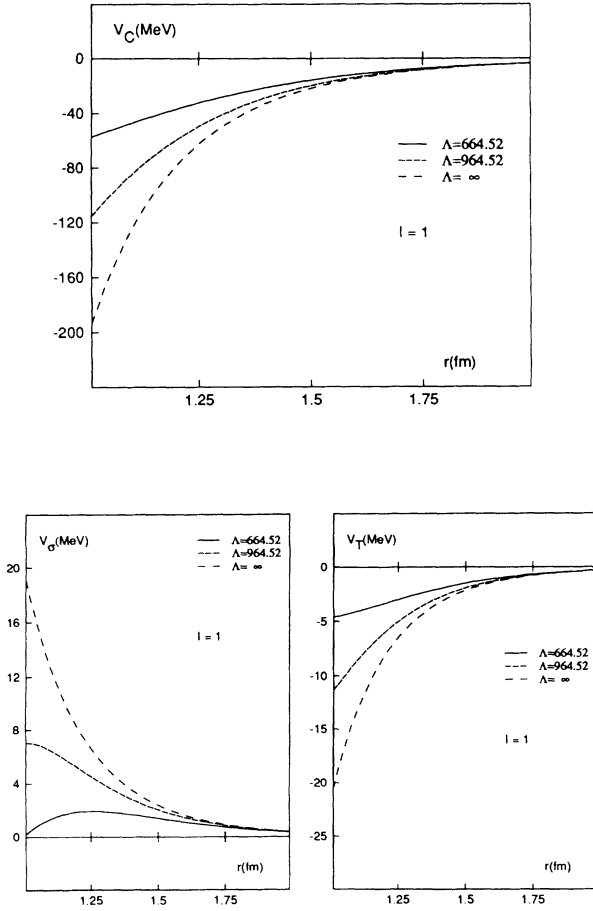
FIG. 16. Dependence of the tail of the central, spin-spin, and tensor potentials on the value of the cutoff mass Λ for $I = 1$.
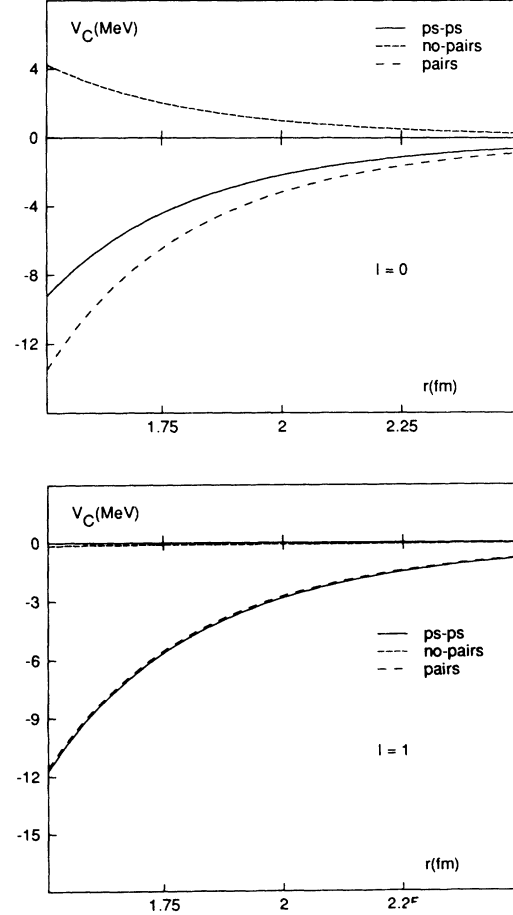
FIG. 17. Influence of the pair terms on the tail of the TPEP with NN intermediate states for (a) $I = 0$ and (b) $I = 1$.

graphs given in Sec. V we use the following identities.

(i) $N\Delta$ graphs. For the evaluation of the contribution due to $D_{//}^{(1)}$ we use

$$\left[\frac{1}{\omega_1}\frac{1}{(\omega_2+a)}+\frac{1}{\omega_2}\frac{1}{(\omega_1+a)}\right]\frac{1}{(\omega_1+\omega_2)}$$
$$=\frac{1}{(\omega_1+a)(\omega_2+a)}\left(\frac{2}{\omega_1+\omega_2}+\frac{a}{\omega_1\omega_2}\right).$$
(B11)

The Fourier transformation of this expression follows from the application of Eqs. (B9) and (B2). The other expressions appearing in the energy denominators can be handled by application of the formulas listed in Eq. (B2).

(ii) $\Delta\Delta$ graphs: The contribution due to $D_{//}^{(2)}$ is the same as Eq. (B11). The expression for $D_X^{(2)}$ is seen from Eq. (5.9) to be of the form

$$\frac{d}{da}\left(\frac{a}{\omega_1\omega_2(\omega_1+a)(\omega_2+a)(\omega_1+\omega_2)}\right.$$
$$\left.+\frac{1}{\omega_1\omega_2(\omega_1+a)(\omega_2+a)}\right).$$
(B12)

Within parentheses there have appeared the by now already familiar expressions discussed in this Appendix. Interchanging the Fourier transformation and the differentiation with respect to the variable a, the evaluation of the corresponding potentials in configuration space is, although a little tedious, straightforward. The evaluation of the various other $D^{(2)}$ expressions poses no problem.

We finally summarize the results of this Appendix by giving a list of the Fourier transforms for the expressions in Eqs. (B2) and (B9). In order to be able to report our results in a somewhat concise form we introduce some convenient notations. First we define

$$\tilde{G}_{n,m}(a,\omega)=\frac{1}{\omega^n}\frac{1}{(\omega+a)^m}.$$
(B13)

From Eq. (B2) the Fourier transforms are seen to be

$$G_{1,0}(a,r)=\frac{2}{\pi}\int_0^\infty d\lambda\,F(\lambda,r),$$
$$G_{0,1}(a,r)=\frac{2}{\pi}\int_0^\infty\frac{\lambda^2 d\lambda}{(a^2+\lambda^2)}\,F(\lambda,r),$$
(B14)
$$G_{1,1}(a,r)=\frac{2a}{\pi}\int_0^\infty\frac{d\lambda}{(a^2+\lambda^2)}\,F(\lambda,r),$$
$$G_{2,1}(a,r)=\frac{1}{a}\left[I_2(m;r)-G_{1,1}(a,r)\right],$$

where $F(\lambda,r)$ was defined in Eq. (B6), and for $m>0$, $G_{n,m+1}(a,r)=-(d/da)G_{n,m}(a,r)$.

Next we define

$$\tilde{H}_{n,m}(a,\omega_1,\omega_2)=\frac{1}{\omega_1^n\omega_2^m}\frac{1}{(\omega_1+a)(\omega_2+a)}\frac{1}{\omega_1+\omega_2}.$$
(B15)

From Eqs. (B9) and (B10) one easily sees that the various Fourier transforms read

$$H_{0,0}(a,r_1,r_2)=\frac{2}{\pi}\int_0^\infty\frac{\lambda^2 d\lambda}{a^2+\lambda^2}\,F(\lambda,r_1)F(\lambda,r_2),$$

$$H_{1,1}(a,r_1,r_2)=\frac{2}{\pi}\int_0^\infty\frac{d\lambda}{a^2+\lambda^2}F(\lambda,r_1)F(\lambda,r_2)$$
$$-\frac{1}{a}G_{1,1}(a,r_1)G_{1,1}(a,r_2),\qquad\text{(B16)}$$

$$H_{2,2}(a,r_1,r_2)=\frac{2}{\pi}\int_0^\infty\frac{d\lambda}{\lambda^2(a^2+\lambda^2)}$$
$$\times[I_2(m,r_1)-F(\lambda,r_1)]$$
$$\times[I_2(m,r_2)-F(\lambda,r_2)].$$

APPENDIX C: CHARACTERISTIC POTENTIAL FORMS

The momentum integrations are carried out as described in Ref. [1]. We write

$$e^{i(\mathbf{k}_1+\mathbf{k}_2)\cdot\mathbf{r}}=\lim_{\mathbf{r}_1,\mathbf{r}_2\to\mathbf{r}}e^{i\mathbf{k}_1\cdot\mathbf{r}_1}e^{i\mathbf{k}_2\cdot\mathbf{r}_2},$$
(C1)

and take the limit operation before the momentum integrations. Then, we replace all momenta occurring in the numerator by ∇_1 and ∇_2 operations, which are the ∇ operations with respect to $\mathbf{r}_1$ and $\mathbf{r}_2$, and take these in front of the momentum integrations. This procedure leads to the following typical forms:

$$\lim_{\mathbf{r}_1\to\mathbf{r}_2}(\nabla_1\cdot\nabla_2)^2F(r_1)G(r_2)=[\nabla_i\nabla_j F(r)]\,[\nabla_i\nabla_j G(r)],$$
(C2)

$$\lim_{\mathbf{r}_1\to\mathbf{r}_2}(\sigma_1\cdot\nabla_1\times\nabla_2)(\sigma_2\cdot\nabla_1\times\nabla_2)F(r_1)G(r_2)$$
$$=\sigma_{1i}\sigma_{2j}\,\epsilon_{ikl}\epsilon_{jmn}\,[\nabla_k\nabla_m F(r)]\,[\nabla_l\nabla_n G(r)],$$
(C3)

where, as usual, we use in this Appendix the convention that repeated indices are summed over. In Eq. (C3) the differentiations work only within the square brackets. For functions depending on r only, one has

$$\nabla_i\nabla_j=O_{ij}^{(1)}\left(\frac{1}{r}\frac{d}{dr}\right)+O_{ij}^{(2)}\left(\frac{d^2}{dr^2}\right),$$
(C4)

$$O_{ij}^{(1)}=\delta_{ij}-\frac{x_i x_j}{r^2},\qquad O_{ij}^{(2)}=\frac{x_i x_j}{r^2}.$$

The tensors $O^{(1)}$ and $O^{(2)}$ satisfy the rules

$$O_{ij}^{(1)}O_{ij}^{(1)}=2,\quad O_{im}^{(1)}O_{jm}^{(1)}=O_{ij}^{(1)},$$
$$O_{ij}^{(1)}O_{ij}^{(2)}=0,\quad O_{im}^{(1)}O_{jm}^{(2)}=0,\qquad\text{(C5)}$$
$$O_{ij}^{(2)}O_{ij}^{(2)}=1,\quad O_{im}^{(2)}O_{jm}^{(2)}=O_{ij}^{(2)}.$$

From these rules it is easy to calculate Eqs. (C2) and (C3). Furthermore, one finds

(i) $\lim\limits_{r_1 \to r_2} (\boldsymbol{\nabla}_1 \cdot \boldsymbol{\nabla}_2)^2 F(r_1)G(r_2) \equiv (F \otimes G)_C (r) = \dfrac{2}{r^2} F'(r)G'(r) + F''(r)G''(r) ,$ $\qquad$ (C6)

(ii) $\lim\limits_{r_1 \to r_2} (\boldsymbol{\sigma}_1 \cdot \boldsymbol{\nabla}_1 \times \boldsymbol{\nabla}_2)(\boldsymbol{\sigma}_2 \cdot \boldsymbol{\nabla}_1 \times \boldsymbol{\nabla}_2) F(r_1)G(r_2) \equiv (F \otimes G)_\sigma (r)(\boldsymbol{\sigma}_1 \cdot \boldsymbol{\sigma}_2) + (F \otimes G)_T (r)S_{12}$

$$= \frac{2}{3} \left[\frac{1}{r^2} F'(r)G'(r) + \frac{1}{r} F'(r)G''(r) + \frac{1}{r} F''(r)G'(r) \right] (\boldsymbol{\sigma}_1 \cdot \boldsymbol{\sigma}_2)$$
$$+ \frac{1}{3} \left[\left(\frac{1}{r} F'(r) - F''(r) \right) \frac{1}{r} G'(r) + \frac{1}{r} F'(r) \left(\frac{1}{r} G'(r) - G''(r) \right) \right] S_{12} , \quad \text{(C7)}$$

(iii) $\lim\limits_{r_1 \to r_2} (\boldsymbol{\nabla}_1 \cdot \boldsymbol{\nabla}_2)(\boldsymbol{\nabla}_1^2 \pm \boldsymbol{\nabla}_2^2) F(r_1)G(r_2) \equiv (F \oslash G)_C^\pm (r) = [(\Delta F)'(r)G'(r) \pm F'(r)(\Delta G)'(r)] ,$ $\qquad$ (C8)

(iv) $\lim\limits_{r_1 \to r_2} (\boldsymbol{\nabla}_1 \cdot \boldsymbol{\nabla}_2)(\boldsymbol{\nabla}_1 \pm \boldsymbol{\nabla}_2) \times \mathbf{Q} \cdot \mathbf{S} \, F(r_1)G(r_2) \equiv (F \oslash G)_1^\pm (r)\mathbf{L} \cdot \mathbf{S} = \dfrac{1}{r} \left[F''(r)G'(r) \pm F'(r)G''(r) \right] \mathbf{L} \cdot \mathbf{S},$

$\qquad$ (C9)

(v) $\lim\limits_{r_1 \to r_2} (\boldsymbol{\nabla}_1 \times \boldsymbol{\nabla}_2) \cdot \mathbf{S}(\boldsymbol{\nabla}_1 \mp \boldsymbol{\nabla}_2) \cdot \mathbf{Q} \, F(r_1)G(r_2) \equiv (F \oslash G)_2^\pm (r)\mathbf{L} \cdot \mathbf{S} = -\dfrac{1 \pm 1}{r^2} F'(r)G'(r)\mathbf{L} \cdot \mathbf{S} .$ $\qquad$ (C10)

The product combinations $(F \otimes G)_C (r), (F \otimes G)_\sigma(r)$, and $(F \otimes G)_T(r)$ introduced above, are used in Sec. V. The product combinations $(F \oslash G)_C (r), (F \oslash G)_1(r)$ and $(F \oslash G)_2(r)$ are used in Sec. VI A.

For the computation of the nonadiabatic corrections of Sec. VI B we need also the higher derivatives. We easily derive (see also Ref. [1], Appendix D)

(vi) $\lim\limits_{r_1 \to r_2} (\boldsymbol{\nabla}_1 \cdot \boldsymbol{\nabla}_2)^3 F(r_1)G(r_2) \equiv (F \odot G)_C (r) = \dfrac{6}{r^2} \left(\dfrac{1}{r} F'(r) - F''(r) \right) \left(\dfrac{1}{r} G'(r) - G''(r) \right) + F'''(r)G'''(r) ,$

$\qquad$ (C11)

(vii) $\lim\limits_{r_1 \to r_2} (\boldsymbol{\nabla}_1 \cdot \boldsymbol{\nabla}_2)(\boldsymbol{\sigma}_1 \cdot \boldsymbol{\nabla}_1 \times \boldsymbol{\nabla}_2)(\boldsymbol{\sigma}_2 \cdot \boldsymbol{\nabla}_1 \times \boldsymbol{\nabla}_2) F(r_1)G(r_2) \equiv (F \odot G)_\sigma (r)(\boldsymbol{\sigma}_1 \cdot \boldsymbol{\sigma}_2) + (F \odot G)_T (r)S_{12}$

$$= -\frac{2}{3} \left[\frac{1}{r^2} \left(\frac{1}{r} F'(r) - F''(r) + rF'''(r) \right) \left(\frac{1}{r} G'(r) - G''(r) + rG'''(r) \right) - F'''(r)G'''(r) \right] (\boldsymbol{\sigma}_1 \cdot \boldsymbol{\sigma}_2)$$
$$+ \frac{1}{3} \left[\frac{1}{r^2} \left(\frac{2}{r} F'(r) - 2F''(r) + \frac{r}{2} F'''(r) \right) \left(\frac{2}{r} G'(r) - 2G''(r) + \frac{r}{2} G'''(r) \right) - \frac{1}{4} F'''(r)G'''(r) \right] S_{12} . \quad \text{(C12)}$$

[1] Th.A. Rijken, Ann. Phys. (N.Y.) **208**, 253 (1991).

[2] M.M. Nagels, Th.A. Rijken, and J.J. de Swart, Phys. Rev. D **17**, 768 (1978).

[3] P.M.M. Maessen, Th.A. Rijken, and J.J. de Swart, Phys. Rev. C **40**, 2226 (1989).

[4] Th.A. Rijken and V.G.J. Stoks, Phys. Rev. C **46**, 102 (1992), the following paper.

[5] H. Sugawara and F. von Hippel, Phys. Rev. **172**, 1764 (1968); *ibid.* **185**, 2046(E) (1969).

[6] A.M. Green and P. Haapakoski, Nucl. Phys. **A221**, 429 (1974).

[7] R.A. Smith and V.R. Pandharipande, Nucl. Phys. **A256**, 327 (1976).

[8] A.M. Green, Rep. Prog. Phys. **39**, 1109 (1976).

[9] M. Chemtob, J.W. Durso, and D.O. Riska, Nucl. Phys. **B38**, 141 (1972).

[10] W.N. Cottingham, M. Lacombe, B. Loiseau, J.M. Richard, and R. Vinh Mau, Phys. Rev. D **8**, 800 (1973).

[11] J.W. Durso, M. Saarela, G.E. Brown, and A.D. Jackson, Nucl. Phys. **A278**, 445 (1977).

[12] R. Machleidt, K. Holinde, and Ch. Elster, Phys. Rep. **149**, 1 (1987).

[13] R. Malfliet and B. ter Haar, Phys. Rep. **149**, 207 (1987).

[14] E.E. van Faassen and J.A. Tjon, Phys. Rev. C **28**, 2354 (1983).

[15] E.L. Lomon, Phys. Rev. D **26**, 576 (1982); P. González and E.L. Lomon, *ibid.* **34**, 1351 (1986).

[16] R.P. Feynman, Phys. Rev. **76**, 769 (1949).

[17] J. Schwinger, Proc. Nat. Acad. Sci. (USA) **37**, 452 (1951).

[18] E. Salpeter and H.A. Bethe, Phys. Rev. **84**, 1232 (1951).

[19] E. Salpeter, Phys. Rev. **87**, 328 (1952).

[20] R.H. Thompson, Phys. Rev. D **1**, 110 (1970).

[21] A. Klein, Phys. Rev. **90**, 1101 (1953).

[22] K.A. Brueckner and K.M. Watson, Phys. Rev. **92**, 1023 (1953), hereafter referred to as BW.

[23] M. Taketani, S. Machida, and S. Ohnuma, Prog. Theor. Phys. (Kyoto) **7**, 45 (1952), hereafter referred to as TMO.

[24] K.A. Brueckner, M. Gell-Mann, and M. Goldberger, Phys. Rev. **90**, 476 (1953); for a discussion and references, see H.A. Bethe and F. de Hoffmann, *Mesons and Fields*, Vol. II *Mesons* (Row, Peterson and Company, New York, 1955).

[25] H.J. Weber and H. Arenhövel, Phys. Rep. C **36**, 277 (1978).

[26] P.A. Carruthers, *Spin and Isospin in Particle Physics* (Gordon and Breach, New York, 1971).

[27] We follow the conventions of J.D. Bjorken and S.D. Drell, *Relativistic Quantum Mechanics* and *Relativistic Quantum Fields* (McGraw-Hill, New York, 1965).

[28] G.E. Brown and W. Weise, Phys. Rep. **C 22**, 281 (1975).

[29] M.M. Lévy, Phys. Rev. **88**, 72 (1952).

[30] From Sec. V on, we use the notation k_1 and k_2 for the momenta of the pions instead of k and k', respectively.

[31] L.T. Thomas, Phil. Mag. **3**, 1 (1927).

[32] R.A.M. Klomp, V.G.J. Stoks, and J.J. de Swart, Phys. Rev. C **44**, R1258 (1991).

[33] R.G.E. Timmermans, Th.A. Rijken, and J.J. de Swart, Phys. Rev. Lett. **67**, 1074 (1991).

[34] M. Sugawara and S. Okubo, Phys. Rev. **117**, 605 (1960); **117**, 611 (1960).

[35] *Handbook of Mathematical Functions*, edited by M. Abramowitz and I. A. Stegun (Dover, New York, 1970).

[36] M.M. Lévy, Phys. Rev. **88**, 725 (1952).